Universitätsklinikum Hamburg-Eppendorf

Zentrum für Experimentelle Medizin
Institut für Neurophysiologie und Pathophysiologie
Direktor: Prof. Dr. Andreas K. Engel

Choice-Induced Biases in Perceptual Decision-Making

Dissertation
zur Erlangung des Doktorgrades PhD
an der Medizinischen Fakultät der Universität Hamburg

vorgelegt von
Anne Eugenia Urai
aus Utrecht

Hamburg, 2018

"Exactly!" said Deep Thought. "So once you do know what the question actually is, you'll know what the answer means."

— *Douglas Adams*, The Hitchhikers' Guide to the Galaxy

Contents

2.1 | Pupil-linked arousal is driven by decision uncertainty and alters serial choice bias

Urai AE, Braun A, Donner TH. (2017) *Nature Communications*, 8:14637

Abstract

While judging their sensory environments, decision-makers seem to use the uncertainty about their choices to guide adjustments of their subsequent behaviour. One possible source of these behavioural adjustments is arousal: Decision uncertainty might drive the brain's arousal systems, which control global brain state and might thereby shape subsequent decision-making. Here, we measure pupil diameter, a proxy for central arousal state, in human observers performing a perceptual choice task of varying difficulty. Pupil dilation, after choice but before external feedback, reflects three hallmark signatures of decision uncertainty derived from a computational model. This increase in pupil-linked arousal boosts observers' tendency to alternate their choice on the subsequent trial. We conclude that decision uncertainty drives rapid changes in pupil-linked arousal state, which shape the serial correlation structure of ongoing choice behaviour.

 doi: 10.1038/ncomms14637. AUTHOR CONTRIBUTIONS: Conceptualization, A.E.U. and T.H.D.; Investigation, A.E.U.; Formal Analysis, A.E.U. and A.B.; Software, data curation and visualization, A.E.U.; Writing, A.E.U. and T.H.D.; Supervision, T.H.D.

Introduction

In perceptual and sensory-motor tasks, humans and animals behave as if they make use of decision uncertainty – the probability that a choice is correct, given the sensory evidence (Kepecs et al. 2008; Ma and Jazayeri 2014; Pouget et al. 2016). Theoretical accounts postulate that decision uncertainty should shape subsequent decision processing and, thereby, subsequent choice behaviour (Kepecs and Mainen 2012; Meyniel et al. 2015; Pouget et al. 2016). But how decision uncertainty is transformed into subsequent behavioural adjustments has, so far, remained elusive.

One prominent idea is that the brain broadcasts uncertainty signals across brain-wide neural circuits via low-level arousal systems (Dayan et al. 2000; Yu and Dayan 2005; Meyniel et al. 2015). Arousal systems might be driven by uncertainty (Aston-Jones and Cohen 2005; Yu and Dayan 2005; Dayan and Yu 2006; Nassar et al. 2012; Meyniel et al. 2015; de Berker et al. 2016), and they profoundly shape the global state of the brain through the action of modulatory neurotransmitters (Harris and Thiele 2011; Lee and Dan 2012; McGinley et al. 2015b). Uncertainty-dependent changes in global brain state, in turn, might translate into adjustments of choice behaviour. The goal of our study was to investigate whether arousal (1) reflects decision uncertainty in a perceptual choice task; and (2) predicts changes in subsequent choice behaviour.

Changes in central arousal state (as assessed by various measures of cortical dynamics) are tightly coupled to fluctuations in pupil diameter under constant luminance (Eldar et al. 2013; Reimer et al. 2014; McGinley et al. 2015a,b; Vinck et al. 2015). We here built on this connection and monitored pupil diameter as a proxy for central arousal state. We used a model based on statistical decision theory, illustrated in Figure 1, in which decision uncertainty is defined as the probability a choice is correct, given the available evidence (Pouget et al. 2016; Sanders et al. 2016). This operationalization of decision uncertainty obviates the need for subjective confidence reports (Kepecs and Mainen 2012), bridging to the insight from animal physiology that neurons in a number of brain regions encode decision uncertainty, as defined in Figure 1 (Kepecs et al. 2008; Komura et al. 2013; Lak et al. 2014; Teichert et al. 2014).

The model assumes that observers base their judgment of each stimulus on a noisy decision variable, sampled from a distribution that depends on the identity and strength of the stimulus (Figure 1a). Two-alternative forced choice tasks entail comparing this decision variable with a decision bound. When the decision variable happens to fall on the wrong side of the bound, errors occur. This happens more often for weaker stimuli, because the distributions corresponding to the two possible stimuli show higher overlap (Figure 1b). A monotonic function of the distance between the decision variable and the bound is a metric of decision confidence; uncertainty is its complement (Kepecs et al. 2008; Hebart et al. 2016; Sanders et al. 2016) (Figure 1a and Methods).

This model predicts three signatures of decision uncertainty (Kepecs et al. 2008; Sanders et al. 2016): (1) uncertainty decreases with evidence strength for correct choices (blue line in Figure 1c) but, counter-intuitively, increases with evidence strength for incorrect choices (red line in Figure 1c); (2) uncertainty predicts a monotonic decrease in choice accuracy from 100 to 50% (Figure 1d); (3) higher uncertainty predicts

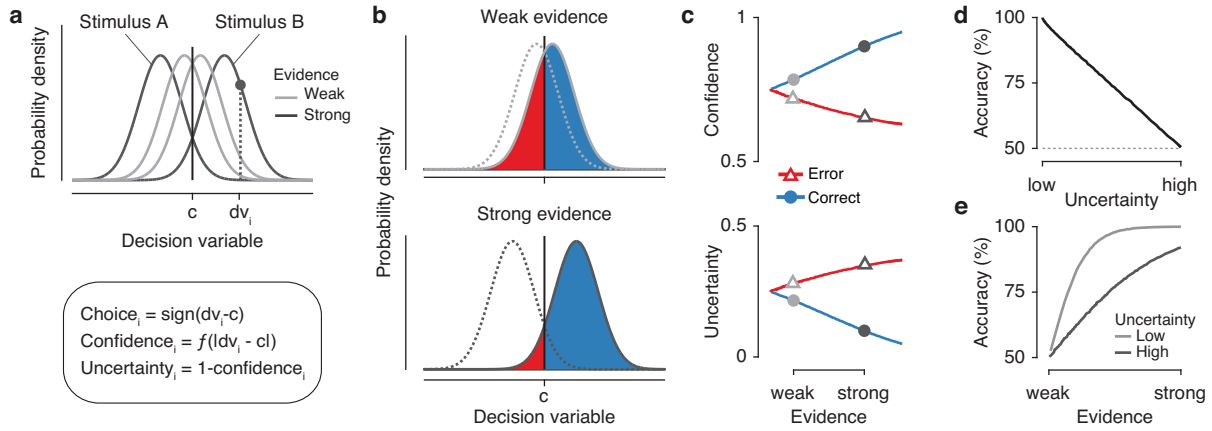

Figure 1. Operationalizing decision uncertainty. (**a**) Computations underlying choice and decision uncertainty. Due to noise, repeated presentations of a generative stimulus produce a normal distribution of internal responses centered at the mean of this generative stimulus. The internal response on each trial dv_i is a sample drawn from this distribution. It is compared to a decision bound or criterion c, to compute the binary choice as well as a graded measure of decision confidence (or its complement: uncertainty). (**b**) For two example levels of evidence strength, the average confidence is indicated by the shaded regions, separately for correct (blue) and error (red) trials. (**c**) Confidence (top) and uncertainty (bottom) as a function of evidence strength (100 bins), separately for correct and error trials. The two levels of evidence indicated by symbols (circles, triangles) correspond to the two example levels of evidence strength in panels **a**, **b**. (**d**) Accuracy as a function of decision uncertainty (100 bins). (**e**) Accuracy as a function of evidence strength (100 bins), separately for trials with high and low decision uncertainty (median split). For details, see Methods and (Kepecs et al. 2008; Sanders et al. 2016).

lower choice accuracy, even for the same evidence strength (Figure 1e). The opposite, monotonic scaling of uncertainty with evidence strength for correct and error trials (Figure 1c) also emerges from a variety of dynamic decision-making models, including race models (Kepecs et al. 2008), Bayesian attractor models (Bitzer et al. 2015), and biophysically detailed circuit models of cortical dynamics (Insabato et al. 2010; Wei and Wang 2015).

We systematically manipulated the strength of sensory evidence and tested whether pupil responses exhibited the three signatures derived above. We then quantified the predictive effects of pupil-linked arousal on subsequent behaviour in terms of the key elements of the perceptual decision process: response time (RT), perceptual sensitivity, lapse rate, and choice bias. Choice bias was decomposed into an overall bias for one choice, and a serial bias dependent on the history of previous choices or stimuli. We found a predictive effect of pupil-linked arousal responses on serial choice bias.

Results

Pupil responses reflect decision uncertainty

27 human observers performed a 2-interval forced choice visual motion coherence discrimination task (Figure 2a and Methods). We applied motion energy filtering (Adelson and Bergen 1985) to the stochastic random dot motion stimuli, yielding a more fine-grained estimate of the decision-relevant sensory evidence contained in the stochastic stimuli than the nominal level of motion coherence (Figure 2b,c and Methods).

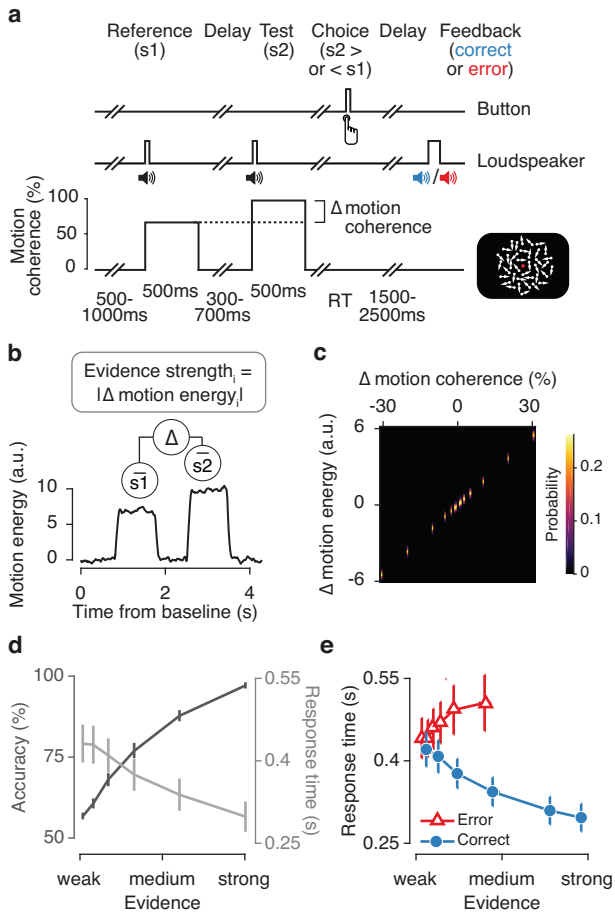

Figure 2. Perceptual choice task and behaviour. (**a**) Behavioural task. Dynamic random dot patterns were displayed throughout each trial. In two successive intervals (onset cued by beeps), the dots moved in one of the four diagonal directions (fixed per observer): A first 'reference' interval with always 70% motion coherence, and a second 'test' interval with varying levels of motion coherence, larger or smaller than the reference. Observers reported whether the test stimulus contained stronger or weaker motion than the reference by pressing one of two buttons. They received auditory feedback after a variable delay. (**b**) Quantifying evidence strength. Each random dot stimulus was convolved with a set of spatio-temporal filters (Adelson and Bergen 1985) to obtain a time course of motion energy. The difference between mean motion energy during test and reference intervals was used as a measure of single-trial measure evidence strength. (**c**) Probability distribution of evidence strength as a function of difference in nominal motion coherence. (**d**) Accuracy and median RT as a function of evidence strength (6 bins). (**e**) Median RT as function of evidence strength (6 bins), split by correct and error trials. (N=27, group mean ± s.e.m.)

The absolute value of this sensory evidence served as a single-trial measure of evidence strength (Figure 2b). As expected, stronger evidence yielded higher choice accuracy and faster responses (Figure 2d and Figure S2a).

In line with previous work (Sanders et al. 2016), RT exhibited all three signatures of decision uncertainty derived in Figure 1 above (Figure 2e and Figure S1b,c). This was true despite the interrogation protocol (Bogacz et al. 2006), in which the test stimulus had a fixed duration, its offset prompted the choice, and observers were instructed to maximize accuracy without speed pressure (response deadline was 3 seconds after test offset). Specifically, RT decreased with evidence strength on correct trials but increased with evidence strength on errors (Figure 2e). Further, RT predicted accuracy over a wide range, but not below

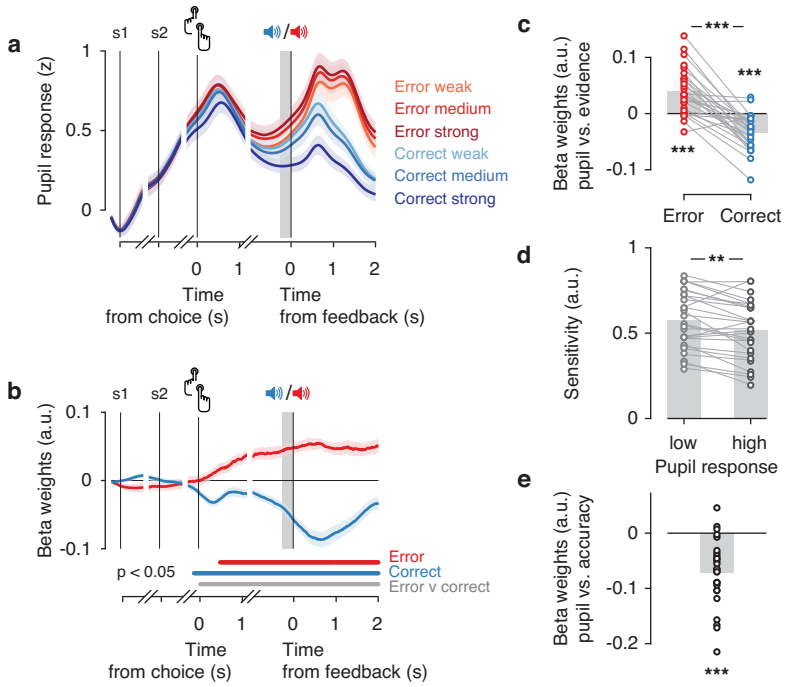

Figure 3. Pupil dilation after choice and before feedback reflects decision uncertainty. (**a**) Time course of pupil responses throughout the trial. Time courses were baseline-corrected and split by correct and error as well as three bins of evidence strength. Mean pupil dilation in the 250 ms before feedback (grey box) was used as a single-trial measure of pupil response. (**b**) Time course of uncertainty scaling in the pupil, computed as sample-by-sample regression of baseline-corrected pupil dilation onto evidence strength. Lower bars indicate $p < 0.05$ from a cluster-corrected permutation test, of the difference between each time course and zero, and between the two time courses. (**c**) Regression weights for the linear relationship between evidence strength and pupil responses. (**d**) Individual perceptual sensitivity, separately for lowest and highest pupil tertiles. (**e**) Individual logistic regression weights, using pupil responses to predict single-trial choice correctness. In **b**-**e** z-scored, log-transformed RTs were removed from the pupil signal via linear regression. *** $p < 0.001$, ** $p < 0.01$, permutation test. (N=27, group mean ± s.e.m.)

50% (Figure S1b), indicating that RT reflected decision uncertainty rather than error detection (Kepecs et al. 2008). We next assessed whether decision uncertainty also affected pupil-linked arousal.

The pupil dilated during decision formation, peaking just after the choice (button press) as observed in previous work (de Gee et al. 2014), and then dilated again after feedback (Figure 3a). Between these two peaks, dilation amplitudes diverged between different conditions, as predicted by decision uncertainty (compare with Figure 1c): Pupil responses were smallest after correct decisions based on strong evidence, they were overall larger after errors than correct choices, and largest after errors made on trials with strong evidence (Figure 3a).

To quantify the temporal evolution of uncertainty scaling in the pupil, we regressed baseline-corrected pupil time courses against each trial's evidence strength, separately for correct and error trials. From choice onwards, pupil dilation scaled positively with evidence strength on error trials, and negatively on correct trials (Figure 3b,c and Figure S3a). In other words, the scaling of the pupil response with evidence strength diagnostic of decision uncertainty emerged in the interval between choice and feedback. Consequently, this uncertainty scaling was not a response to the external information about choice correctness provided by the

external feedback, but rather reflected internal decision-related computations as described in Figure 1. For simplicity, we refer to the single-trial pupil dilation averaged across the 250 ms interval before feedback as 'pupil response' in the following.

The pupil response also exhibited the other two signatures of decision uncertainty predicted by the model in Figure 1. Larger pupil responses were accompanied by an overall lower choice accuracy (Figure 3e and Figure S3c), and psychophysical sensitivity was lower on trials with a larger pupil response (Figure 3d and Figure S3b). Specifically, the pupil response did not predict choice accuracy below 50%, suggesting that it did not signal the detection of errors (Figure S3c).

The scaling of the pupil response with decision uncertainty was not inherited from the analogous scaling of RT, but was also present after first removing (via linear regression) the trial-to-trial variations accounted for by RT (Figure S3d-f). Indeed, trial-to-trial correlations between pupil responses and RTs were generally small (Pearson correlation, average r: 0.087 range: -0.042 to 0.302, for log-transformed RT). For all subsequent analyses reported in this paper, we removed RT-fluctuations from the trial-to-trial fluctuations of single-trial pupil responses via linear regression (see Methods).

Pupil-linked arousal alters subsequent choice behaviour

We proceeded to test whether uncertainty-related pupil responses predicted changes in subsequent choice behaviour. It has been proposed that arousal signals control various aspects of learning and decision-making (Dayan et al. 2000; Aston-Jones and Cohen 2005; Yu and Dayan 2005; Dayan and Yu 2006; Meyniel et al. 2015). In the context of our task, the choice parameters of interest were perceptual sensitivity (measured as the slope of the psychometric function, Figure S4a), lapse rate (measured as the vertical distance of the asymptotes of the psychometric function from 0 or 1, Figure S4a), bias (measured as the horizontal shift of the psychometric function, Figure S4a), and RT. For RT, we focussed on increases after error trials, an effect referred to as post-error slowing (Dutilh et al. 2012), which was found to be modulated by pupil-linked arousal in a speeded RT task (Murphy et al. 2016b). Choice bias was further decomposed into two parameters: overall bias (i.e., a general tendency towards one choice option, averaged across the entire experiment, Figure S4b) and serial bias (i.e., a local, choice history-dependent tendency towards one option that becomes evident when conditioning the psychometric function on the preceding choice, Figure S4c) (Fernberger 1920; Yu and Cohen 2008; Fründ et al. 2014). Because in our task (as common in laboratory choice tasks), the sensory evidence was independent across trials, any serial bias was maladaptive, reducing observers' performance below the optimum they could achieve given their perceptual sensitivity.

The pupil response predicted a reduction of serial choice bias (Figure 4a and Figure S5). When a choice was followed by a small pupil response, observers tended to repeat this choice on the next trial; when the previous pupil response was large, this serial bias was abolished (Figure 4a). This predictive effect was similar for correct and error trials (Figure S6a). An analogous pattern of predictive effects was observed when binning by previous trial RT: Fast, but not slow, RTs were followed by a tendency to repeat the previous choice

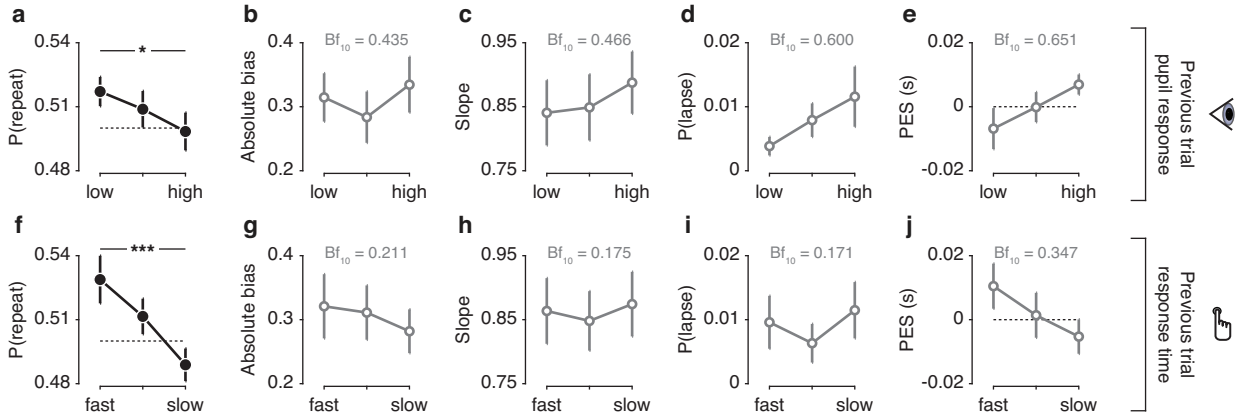

Figure 4. Pupil responses and RT predict reductions in serial choice bias. (**a**) Serial choice bias, quantified as the history-dependent shift of the psychometric function, for tertiles of previous trial pupil responses. (**b**) Absolute choice bias, measured as the intercept of a logistic psychometric function, for tertiles of previous trial pupil responses. (**c**) Perceptual sensitivity, measured as the slope of a logistic psychometric function, for tertiles of previous trial pupil responses. (**d**) Lapse rate, measured as the probability of stimulus-independent guesses, for tertiles of previous trial pupil responses. (**e**) Post-error slowing, for tertiles of previous trial pupil responses. (**f**-**j**) as in **a**-**e**, but for tertiles of previous trial RT. *** $p < 0.001$, * $p < 0.05$, main effect of pupil/RT bin on repetition probability computed from a one-way repeated measures ANOVA. Unfilled markers indicate $p > 0.05$, with Bf_{10} from a Bayesian repeated measures ANOVA written in panel. (N=27, group mean ± s.e.m.)

(Figure 4f and Figure S6b).

The pupil response predicted none of the other choice parameters on the next trial (assessed by one-way repeated measures ANOVA), neither overall choice bias (signed overall bias: $F_{(2,52)} = 0.939$, $p = 0.398$, $Bf_{10} = 0.221$; absolute value of overall bias: $F_{(2,52)} = 1.817$, $p = 0.173$, Figure 4b), nor perceptual sensitivity ($F_{(2,52)} = 1.936$, $p = 0.155$, Figure 4c), nor lapse rate ($F_{(2,52)} = 2.213$, $p = 0.120$, Figure 4d), nor RT (overall RT: $F_{(2,52)} = 3.232$, $p = 0.048$, $Bf_{10} = 1.207$; post-error slowing: $F_{(2,52)} = 2.056$, $p = 0.138$, Figure 4e). Variations in RT, likewise, did not predict a change in any of the other parameters of the decision process (Figure 4g-j, all $p > 0.05$). The overall pattern of results implies that observers did not simply act more randomly after large pupil responses or RT. Random button presses would have reduced sensitivity, in other words, decreased the slope of the psychometric function, contrary to our observations (Figure 4c,h). Rather, the pattern of results implies that, after large pupil responses or RT, observers' tendency towards one or the other choice became less history-dependent.

In sum, large pupil responses and slow RTs were neither followed by improved processing of sensory evidence (a common effect of attention, Ress et al. 2000), nor a change in overall response bias. Large pupil responses and slow RTs were followed by only minor (and statistically not significant) changes in stimulus-independent lapses as well as small adjustments in speed accuracy trade-off, as observed after response conflict, errors, or large pupil responses in speeded RT tasks (Botvinick et al. 2001; Gao et al. 2009; Murphy et al. 2016b). The weak effect on post-error slowing might be due to the use of an interrogation protocol in our study, which did not require observers to optimize their speed-accuracy trade-off (Bogacz et al. 2006). However, both RT and pupil-linked arousal had a robust effect on serial choice bias, reducing an overall repetition bias that predominated across the group of observers. This effect of both uncertainty-related

measures on the serial correlation structure of choice behaviour has so far been unknown. We therefore proceeded to model and comprehensively quantify this effect at the level of individual observers.

Pupil-linked arousal predicts choice alternation

To this end, we extended a previously established regression model of serial choice biases (Fründ et al. 2014) with pupil- and RT-dependent modulatory effects. The basic model (i.e., without modulatory terms) quantified the impact of the previous seven choices and stimuli on the current choice bias in terms of linear combination weights (Figure 5a, see Methods and (Fründ et al. 2014). We added to this model multiplicative interaction terms, that quantified how much the effect of previous stimuli and choices was modulated by either pupil response or RT on those same trials (Figure 5a). Simultaneously modeling the effects of both pupil responses and RT enabled us to estimate their independent impact on serial choice bias; we found the same results when fitting a separate regression model for each modulatory variable (Figure S7).

The model fits revealed robust, and idiosyncratic, patterns of serial choice biases in most observers (Figure 5c,d; see Figure S2b,c for individual sessions). As expected, the contribution of past stimuli and choices to current behaviour was strongest when sensory evidence was weak and decayed strongly with evidence strength (Figure 5b). The weight of the immediately preceding choice was generally stronger than the weight of the previous stimulus (Figure 5d). The effect of previous choices lasted up to seven trials in the past (corresponding to about 60 s, Figure 5c), but had the largest absolute magnitude on the preceding trial (Figure 5c, grey dashed line). There was large inter-individual variability in choice weights (Figure 5c,d). While the majority of observers systematically repeated their choices (purple symbols; 12 significant at $p < 0.05$), a good fraction tended to alternate their choices (orange symbols; 7 significant at $p < 0.05$).

Observers' serial choices biases were unrelated to the (small) serial correlations between stimuli. The transition probabilities between stimulus categories (i.e. s2<s1 or s2>s1) were close to 0.5 (range across observers: 0.475 to 0.508), and did not correlate with individual choice weights (Pearson correlation $r = 0.010$, $p = 0.960$, $Bf_{10} = 0.149$) or stimulus weights (Pearson correlation $r = -0.176$, $p = 0.381$, $Bf_{10} = 0.217$). Likewise, the auto-correlation of absolute motion coherence differences (i.e., absolute levels of evidence strength) was close to 0 (range across observers: -0.061 to 0.028) and did not correlate with individual choice weights (Pearson correlation $r = 0.123$, $p = 0.541$, $Bf_{10} = 0.179$) or stimulus weights (Pearson correlation $r = -0.142$, $p = 0.480$, $Bf_{10} = 0.190$).

Critically, pupil responses and RT both negatively interacted with the effect of previous choices (Figure 5e), in line with the observation that large pupil responses or long RTs were followed by less choice repetition (Figure 4a,f). By contrast, neither pupil responses nor RT interacted with the effect of the previous stimulus (Figure 5e). Pupil responses beyond one trial in the past, as well as baseline pupil diameter on the current trial, did not predict a modulation of serial biases (Figure S8). Moreover, these results were not accounted for by trial-to-trial variations in trial timing or the passage of time between trials (Figure S9).

The pupil response after feedback did not contain information predictive of serial choice bias, beyond the

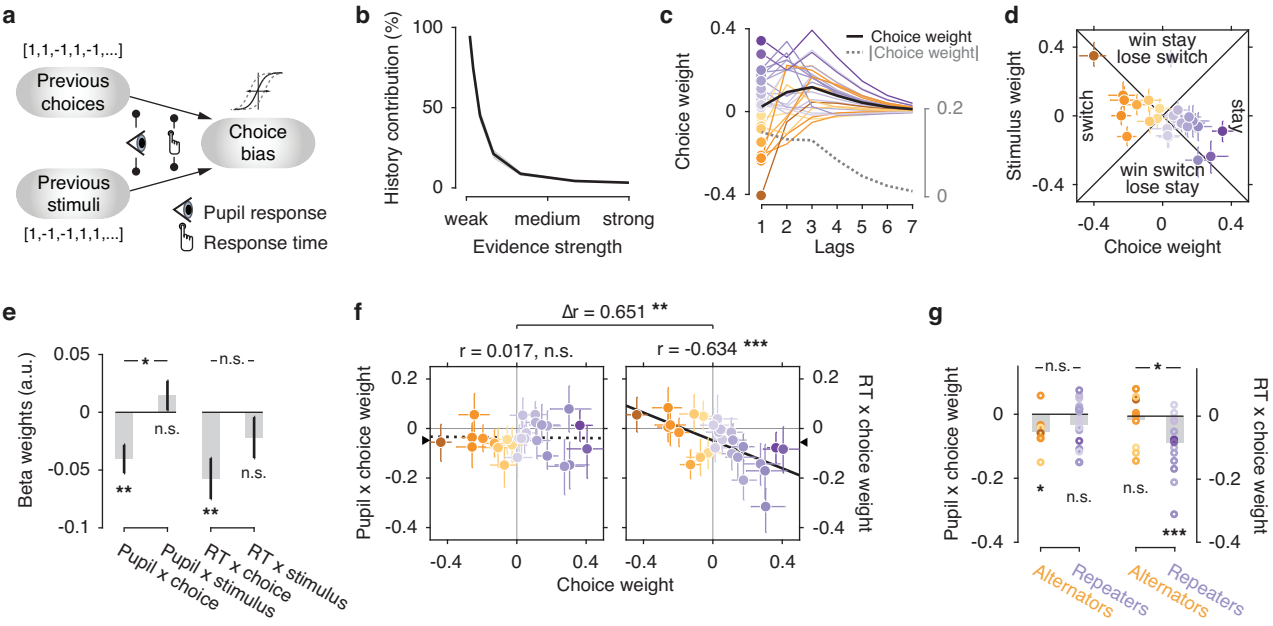

Figure 5. Modeling the modulation of serial choice bias. (**a**) Schematic of the regression model with modulatory terms. (**b**) The contribution of history terms (past choices and stimuli) as a fraction of the total variance in the decision variable (Fründ et al. 2014), decreased with stronger sensory evidence. (**c**) Choice weights for the previous 7 trials, obtained from the history model without modulatory terms. Each line corresponds to one observer. Purple, 'repeaters' with positive choice weight for lag 1. Orange, 'alternators' with negative choice weights for lag 1. Black line, group mean. Grey dashed line, group mean of absolute choice weight. (**d**) Choice weights at lag 1 plotted against the corresponding stimulus weights. Colored dots and error bars indicate individual observers ± 68% confidence intervals obtained from a bootstrap. See Methods for an interpretation of this graph in terms of behavioural strategy. (**e**) Regression weights for the interaction between previous pupil response or RT and previous choices or stimuli. N=27, group mean ± s.e.m. (**f**) Correlation between choice weights and their modulation by pupil dilation or RT. Colors indicate the choice weight as derived from the basic model in **d**. Error bars are 68% confidence intervals obtained from a bootstrap. The intercept of the least-squares regression line, corresponding to the mean beta weight across the group, is indicated with a triangle on the y-axis. (**g**) Beta weights for interaction between previous pupil response or RT and previous choices. Group split based on the sign of individual choice weights. *** $p < 0.001$, ** $p < 0.01$, * $p < 0.05$, n.s. $p > 0.05$, Pearson's correlation coefficient or permutation test.

information already present during the pre-feedback interval. The post-feedback pupil responses similarly predicted modulation of serial choice biases, but no longer did so when removing (via linear regression) variance explained by pre-feedback pupil responses from the post-feedback pupil signal (Figure S10).

While the modulatory effects associated with pupil responses and RT were both negative on average, such an overall reduction of the group-level repetition bias (Figure 4a,f) might be due to two alternative scenarios at the level of individual observers: either a reduction of each observer's intrinsic serial choice bias for repetition or alternation (referred to as 'bias reduction' hereafter); or, alternatively, a general boost of choice alternation, regardless of the observer's intrinsic serial bias (referred to as 'alternation boost'). We quantified intrinsic serial bias as each observer's choice weight (i.e., the main effect of the previous on the current choice estimated by our model). The bias reduction scenario predicts a negative correlation between choice weights and modulation weights across observers. The alternation boost scenario predicts negative individual modulation weights for all observers, independently of their corresponding choice weights (i.e., no correlation).

The analysis of these individual behavioural patterns revealed dissociable effects of pupil-linked arousal and RT (Figure 5f,g). Modulation weights for the pupil were negative for most observers, irrespective of their individual choice weight. When splitting all 27 observers into 'alternators' and 'repeaters' based on the sign of their intrinsic bias (i.e., choice weight), we found no correlation between individual modulation and choice weights (Figure 5f, Pearson correlation r = -0.017, p = 0.935, Bf_{10} = 0.149). Further, the modulation weights were negative for both subgroups, and not significantly different between them (Figure 5g). These observations are consistent with the idea that pupil-linked arousal generally boosted observers' tendency to alternate their choice on the next trial.

The alternation boost scenario for pupil responses was further supported by a striking contrast to RT-linked modulations, which were in line with the bias reduction scenario. The RT-linked modulation weights exhibited a strong negative correlation with individual choice weights (Figure 5f, Pearson correlation r = -0.634, p < 0.001, Bf_{10}= 76.359), were negative only for the group of repeaters, and differed significantly between alternators and repeaters (Figure 5g). Correspondingly, the correlations with individual choice weights were significantly different for pupil- and RT-modulation weights (Figure 5f). Moreover, RT-dependent bias reduction was most pronounced after incorrect choices, whereas the pupil-dependent alternation boost was most pronounced after correct choices (Figure S11).

In sum, the modulatory effects associated with post-decision pupil-linked arousal and RT both shaped the serial correlation structure of choices, but in distinct ways: pupil-linked arousal generally promoted choice alternation, regardless of the observer's intrinsic bias, whereas RT-linked processes generally reduced observers' intrinsic bias.

Discussion

Decisions about an observer's sensory environment do not only depend on the momentary sensory input, but also on the behavioural context (Gold and Shadlen 2007). One such contextual factor is the history of preceding choices and stimuli, which robustly biases even highly trained decision-makers (Fründ et al. 2014). Although such serial choice biases were first identified in psychophysical tasks about a century ago (Fernberger 1920), their determinants have remained poorly understood. Previous treatments of serial choice biases have conceptualized experimental history as sequences of binary external events (past stimulus identities, choices, or feedback) (Fründ et al. 2014; Abrahamyan et al. 2016). We here established that these serial biases were also modulated by the decision-maker's pupil-linked arousal state on the previous trial, which, in turn, reflected the uncertainty about the observer's choice.

Several important features of our approach allowed us to move beyond previous work linking human pupil dynamics to uncertainty and performance monitoring. First, different from most previous studies, we here unravelled the temporal evolution of uncertainty information in the pupil response, enabling inferences about not only the existence, but also the time course of this information (see O'Reilly et al. 2013 for a similar approach). Second, the model-based definition of decision uncertainty we used helped dissociate decision

uncertainty from error detection, which has previously been linked to pupil dilation (Wessel et al. 2011). In a two-choice task, a signal encoding decision uncertainty should predict behavioural performance over a range from 100% to 50% correct (corresponding to 50% for the maximum uncertainty signal, or larger when encoding is imprecise). By contrast, an error detection signal should predict performance over the range 100% to 0% correct (Kepecs et al. 2008). Our measurements were more consistent with decision uncertainty than error detection (Figure S3c). Third, in our task, decision uncertainty critically depended on internal noise (the primary source of the variance in Figure 1a). By contrast, previous studies linking uncertainty to pupil dynamics (Preuschoff et al. 2011; Nassar et al. 2012; O'Reilly et al. 2013; de Berker et al. 2016) have used tasks in which the primary source of uncertainty was in the observers' environment. Last, in contrast to most previous pupillometry studies (Preuschoff et al. 2011; de Gee et al. 2014; Lempert et al. 2015) we comprehensively quantified the predictive effects of pupil-linked arousal on the parameters of choice beyond the current trial, thereby complementing recent work on the effects of pupil-linked arousal on learning (Nassar et al. 2012; O'Reilly et al. 2013). Taken together, our results critically advance the understanding of how internal decision uncertainty is encoded in pupil-linked arousal in humans, in a way that builds a direct bridge to single-unit recording studies of decision uncertainty in animals (Kepecs et al. 2008; Komura et al. 2013; Lak et al. 2014; Teichert et al. 2014).

The neural sources of task-evoked pupil responses at constant luminance are not yet fully identified (McDougal and Gamlin 2008), but mounting evidence points to the noradrenergic locus coeruleus (LC) (Murphy et al. 2014; Varazzani et al. 2015; Joshi et al. 2016) (a core component of the brain's arousal system (Aston-Jones and Cohen 2005)) as well as the superior and inferior colliculi (Wang et al. 2015). Microstimulation of all three structures triggers pupil dilation (Joshi et al. 2016). Among these structures, activity of the LC (spontaneous or evoked by electrical stimulation) is followed by pupil dilation at the shortest latency (Joshi et al. 2016). The LC also has widespread, modulatory projections to the cortex implicated in regulating central arousal (Aston-Jones and Cohen 2005). Dopaminergic and cholinergic systems, which are closely connected with the LC (Sara 2009), are likewise implicated in central arousal state (McGinley et al. 2015b) and may also contribute to task-evoked pupil responses.

We propose that decision-makers' uncertainty about their choices might shape serial choice biases by recruiting pupil-linked neuromodulatory systems. Frontal brain regions encoding decision uncertainty send descending projections to several of these systems (Aston-Jones and Cohen 2005; Sara 2009), which in turn project to large parts of the cortex, including networks of regions involved in perceptual inference and decision-making (Siegel et al. 2011). Neuromodulators like noradrenaline can profoundly alter the dynamics and topology of cortical networks (Marder 2012; Eldar et al. 2013; Polack et al. 2013; McGinley et al. 2015b). Thus, these brainstem arousal systems might be in an ideal position to transform variations in decision uncertainty into adjustments of choice behaviour (Yu and Dayan 2005; Meyniel et al. 2015).

The behavioural effect of pupil-linked arousal might be explained by at least two (not mutually exclusive) scenarios. First, arousal responses might promote choice alternation at the level of response preparation, by altering the state of the motor system (de Lange et al. 2013). Second, the arousal response might modulate

the decision stage – specifically the dynamic updating of beliefs about the upcoming evidence, for example by shifting the criterion (assumed to be constant in signal detection theory, Figure 1) from one choice to the next. When this criterion is shifted in the direction opposite to the last choice, alternation ensues. In line with these ideas, changes in pupil-linked arousal state can indeed translate into specific behavioural effects (Eldar et al. 2013; de Gee et al. 2014), presumably by interacting with selective cortical circuitry (Donner et al. 2013).

Our current observations are not easily reconciled with existing theoretical accounts of the impact of phasic arousal on decision-making. One account posits that threshold crossing of the decision variable triggers phasic noradrenaline release, facilitating the translation of the decision into a behavioural response (Aston-Jones and Cohen 2005). In contrast to our observations, this framework focuses on functional effects of phasic arousal within the same trial, rather than subsequent ones, and it predicts improvements in sensitivity and/or RT (Cavanagh et al. 2014), rather than changes in bias. Other accounts have proposed that phasic noradrenaline release facilitates a 'network reset' (Bouret and Sara 2005), enabling the transition of neural decision circuits to a new state (Dayan and Yu 2006). Our group-level finding that high pupil-linked arousal reduces serial biases might be interpreted as the discarding of post-decisional activity traces due to network reset (Karlsson et al. 2012; Tervo et al. 2014). However, our analysis of individual choice patterns revealed that pupil-linked arousal boosted alternation also in those observers who already exhibited a tendency to alternate their choices, which is not easily reconciled with the network reset idea.

Previous theories of arousal and neuromodulation have coarsely distinguished between two timescales of arousal fluctuations: Tonic fluctuations over the course of seconds to hours, and phasic responses on a sub-second timescale, time-locked to rapid cognitive acts (Aston-Jones and Cohen 2005; Yu and Dayan 2005; Dayan and Yu 2006). Changes in tonic arousal occur spontaneously (Steriade 2000; McGinley et al. 2015b), and might also track changes in task utility or uncertainty (Aston-Jones and Cohen 2005; Yu and Dayan 2005; Nassar et al. 2012; de Berker et al. 2016). Pupil-linked changes in tonic arousal strongly shape the operating mode of cortical circuits, including early sensory cortices, on slow timescales (McGinley et al. 2015b). Phasic pupil-linked arousal responses, on the other hand, predict behaviour related to the same transient cognitive processes that drive them (Einhäuser et al. 2008; Preuschoff et al. 2011; de Gee et al. 2014). The uncertainty-linked pupil responses we identified here built up slowly after choice and predicted choice behaviour several seconds later. Thus, our current results suggest that pupil-linked arousal systems are driven by, and interact with, cognitive processes also at intermediate timescales; faster than tonic arousal, but more sustained than task-evoked phasic responses.

The dissociation between pupil- and RT-linked modulatory effects (Figure 5f and Figure S11) on serial choice bias suggests that decision uncertainty signals were propagated along distinct central neural pathways, one linked to pupil responses and the other to RT, which then shaped serial choice biases in different ways. Even if the same uncertainty signals fed into these pathways, they might have become decoupled through independent internal noise. Specifically, it is tempting to speculate that the pupil-linked alternation boost reflected neuromodulator release from brainstem centers (such as noradrenaline from the LC, Tervo

et al. 2014), whereas RT-linked bias reduction was driven by frontal cortical areas involved in explicit performance monitoring and top-down control (such as anterior cingulate cortex, Botvinick et al. 2001; Yeung et al. 2004; Ebitz and Platt 2015). Top-down effects of prefrontal cortex on decision-making (Botvinick et al. 2001; Miller and Cohen 2001) are commonly associated with explicit strategic effects that are adaptive within the experimental task. Indeed, the RT-linked modulation of serial bias was adaptive, in that it generally reduced observers' intrinsic serial bias. By contrast, pupil-linked arousal modulated serial choice patterns in a way that was maladaptive for part of the observers (the alternators). This finding might be related to the observation that maladaptive serial choice biases remain prevalent even in highly trained observers who know the statistics of the task (Fernberger 1920; Fründ et al. 2014). Taken together, the dissociation between pupil- and RT-linked effects suggest that serial choice biases result from a complex interplay between low-level, pupil-linked arousal systems and higher-level systems for strategic control. Future studies should pinpoint the neural systems underlying these distinct effects, as well as their interactions (Tervo et al. 2014).

In conclusion, our study identified decision uncertainty as a high-level driver of phasic arousal, and it uncovered a role of this pupil-linked arousal response in shaping the dynamics of serial choice biases – a pervasive but often ignored characteristic of human decision-making. These insights shed new light on the link between decision uncertainty, pupil-linked arousal state, and serial dependencies in decision-making. They set the stage for further investigations into the neural bases of arousal-dependent modulations of serial choice behaviour.

Methods

Operationalizing decision uncertainty

In signal detection theory, a decision variable dv_i is drawn on each trial from a normal distribution $\mathcal{N}(\mu, \sigma)$ with μ corresponding to that trial's sensory evidence and σ reflecting the internal noise. In Figure 1, we used the range of single-trial motion energy values $[-6, 6]$ as our μ. We estimated σ from the data using a probit psychometric function fit on data combined across observers. The probit slope $\beta = 0.367$, where its inverse $\sigma = 2.723$ reflected the standard deviation of the dv distribution. The decision bound c was set to 0, reflecting an observer without overall choice bias. The two pairs of distributions in Figure 1 were generated using $\mu = -1$ and $\mu = 1$ for weak evidence, and $\mu = -4$ and $\mu = 4$ for strong evidence. To calculate the relationship between evidence strength and decision uncertainty (Figure 1c), we simulated a normal distribution of dv for each level of evidence strength, with $\mu = [0, 6]$ and $\sigma = 2.723$. Since these uncertainty computations are symmetrical with respect to choice identity, we visualized only the pattern corresponding to $\mu > 0$ (stimulus B in Figure 1a). All samples from such a distribution were split into correct and error parts based on their position with respect to the decision bound c. For each combination of evidence strength and choice, the average uncertainty level is w

$$uncertainty = 1 - \frac{1}{n}\sum_{i=1}^{n} f(|dv - c|) \quad (1)$$

where f is the cumulative distribution function of the normal distribution

$$f(x) = \frac{1}{2}\left[1 + \text{erf}\left(\frac{x}{\sigma\sqrt{2}}\right)\right] \quad (2)$$

which transforms the distance between dv and c into the probability of a correct response (Lak et al. 2014).

We simulated ten million trials based on the range of evidence in the data, and for each we computed a binary choice, the corresponding level of decision uncertainty, and the accuracy of the choice. Figure 1c-e visualises the relationship between evidence strength, uncertainty and choice accuracy in these simulated data.

Participants and sample size

Twenty-seven healthy human observers (10 male, aged 23 $\pm$ 5.2 years) participated in the study. The ethics committee at the University of Amsterdam approved the study, and all observers gave their informed consent. We included all observers in each analyses presented in the paper. Each observer participated in one practice session and five main experimental sessions, each of approximately two hours and comprising 500 trials of the task. The number of observers was selected to allow for robust analyses of individual differences, as in previous pupillometry work from our lab (de Gee et al. 2014), and the total number of trials per observer was chosen to allow for robust psychometric function fits and detection of subtle changes in the fit parameters.

Task and procedure

Observers performed a 2-interval forced choice motion coherence discrimination task at constant luminance (Figure 2a). Observers judged the difference in motion coherence between two successively presented random dot kinematograms (RDKs): a constant reference stimulus (70% motion coherence) and a test stimulus (varying motion coherence levels specified below). The intervals before, in between, and after (until the inter-trial interval) these two task-relevant stimuli had variable duration (numbers in Figure 2a) and contained incoherent motion. A beep (50 ms, 440 Hz) indicated the onset of each (test and reference) stimulus. After offset of the test stimulus, observers had 3 seconds to report their judgment (button press with left or right index finger, counterbalanced across observers). After a variable interval (1.5-2.5 s), a feedback tone was played (150 ms, 880 Hz or 200 Hz, feedback-tone mapping counterbalanced across observers). Dot motion was stopped 2-2.5 s after feedback, with stationary dots indicating the inter-trial interval, during which observers were allowed to blink their eyes. Observers self-initiated the next trial by button press (range of median inter-trial intervals across observers: 0.68 to 2.05 s).

The difference between motion coherence of test and reference was taken from three sets: easy (2.5, 5, 10, 20, 30), medium (1.25, 2.5, 5, 10, 30) and hard (0.625, 1.25, 2.5, 5, 20). All observers started with the easy set. We switched to the medium set when their psychophysical thresholds (70% accuracy defined by a

cumulative Weibull fit) dropped below 15%, and to the hard set when thresholds dropped below 10%, in a given session.

Motion coherence differences were randomly shuffled within each block. We applied a counterbalancing scheme ensuring that within a block, each stimulus category (s2 > or < s1) was followed by itself or its opposite equally often (Brooks 2012). The algorithm generated sequences of 53 trials, of which the first 50 were used per block.

Random dot kinematograms

Stimuli were generated using PsychToolbox-3 (Kleiner et al. 2007) and presented on a 22" CRT monitor with a resolution of 1024 x 768 pixels and a refresh rate of 60 Hz. A red 'bulls-eye' fixation target (Thaler et al. 2013) of 1.5° diameter was present in the centre of the screen. Dynamic random noise was presented in a central annulus (outer radius 12°, inner radius 2°) around fixation. The annulus was defined by a field of dots with a density of 1.7 dots/degrees^2, resulting in 768 dots on the screen in any given frame. Dots were 0.2° in diameter and had 100% contrast from the black screen background. All dots were divided into 'signal dots' and 'noise dots', whose proportions defined the varying motion coherence levels. Signal dots were randomly selected on each frame, and moved with 11.5°/s in one of four diagonal directions (counterbalanced across observers). Signal dots that left the annulus wrapped around and reappeared on the other side. Signal dots had a limited 'lifetime' and were re-plotted in a random location after being on the screen for 4 consecutive frames. Noise dots were assigned a random location within the annulus on each frame, resulting in 'random position noise with a 'different' rule (Scase et al. 1996). Three independent motion sequences were interleaved (Roitman and Shadlen 2002), making the effective speed of signal dots in the display 3.8°/s.

Motion energy filtering

Due to the stochastic nature of the dynamic random dot kinematograms, the sensory evidence fluctuated within and across trials, around the nominal motion coherence level. To quantify behaviour and pupil responses as a function of the actual, rather than the nominal, single-trial evidence, we used motion energy filtering to estimate those fluctuations (Adelson and Bergen 1985).

Two spatial filters, resembling weighted sinusoids in opposite phase, were defined by

$$f_1(x, y) = \cos^4(a)\cos(4a)\exp(-\frac{y'^2}{2\sigma_g^2}) \tag{3}$$

$$f_2(x, y) = \cos^4(a)\sin(4a)\exp(-\frac{y'^2}{2\sigma_g^2}) \tag{4}$$

where $a = \tan^{-1}(x'/\sigma_c)$. The parameters $\sigma_g = 0.05$ and $\sigma_c = 0.35$ defined the carrier sinusoid and the Gaussian envelope, respectively, in line with the response properties of MT neurons (Kiani et al. 2008).

The coordinate system (x, y) was rotated to match the stimulus' target direction or its 180° opposite. Two temporal filters were defined by

$$g_1(t) = (kt)^{n_s} \exp(-kt) \left[\frac{1}{n_s!} - \frac{(kt)^2}{(n_s+2)!}\right] \quad (5)$$

$$g_2(t) = (kt)^{n_f} \exp(-kt) \left[\frac{1}{n_f!} - \frac{(kt)^2}{(n_f+2)!}\right] \quad (6)$$

Where $k = 60$ reflected the envelope of the temporal filters, and $n_s = 3$ and $n_f = 5$ controlled the width of the slow and fast filters, respectively (Kiani et al. 2008). A pair of spatio-temporal filters in quadrature pair was obtained by $f_1 g_1 + f_2 g_2$ and $f_2 g_1 - f_1 g_2$. We convolved each filter with the single-trial random dot movies. The resulting values were squared, and summed together across the two filters (Adelson and Bergen 1985).

This filtering procedure was performed for each observer's individual target direction as well as its 180° opposite. To avoid cardinal biases in motion perception, we used the four diagonals as target directions counterbalanced across observers. Outputs of the two filtering operations were subtracted to yield a direction-selective signal over time (Kiani et al. 2008). To obtain a single measure of sensory evidence per trial, we averaged over all timepoints within each stimulus interval, and took the difference between motion energy in the first and second interval as our measure of single-trial sensory evidence. Evidence strength was defined by taking the absolute value of this sensory evidence, collapsing over the two stimulus identities (Figure 2b).

Pupillometry

Observers sat in a dark room with their head in a chinrest at 50 cm from the screen. Horizontal and vertical gaze position, as well as the area of the pupil, were monitored in the left eye using an EyeLink 1000 desktop mount (SR Research, sampling rate: 1,000 Hz). The eye tracker was calibrated before each block of 50 trials.

Missing data and blinks, as detected by the EyeLink software, were padded by 150 ms and linearly interpolated. Additional blinks were found using peak detection on the velocity of the pupil signal and linearly interpolated. We estimated the effect of blinks and saccades on the pupil response through deconvolution, and removed these responses from the data using linear regression using a procedure detailed in ref (Knapen et al. 2016). The residual pupil time series were band-pass filtered using a 0.01 to 10 Hz second-order Butterworth filter, z-scored per run, and resampled to 100 Hz. We epoched trials, and baseline corrected each trial by subtracting the mean pupil diameter 500 ms before onset of the reference stimulus.

We included all trials from all five main sessions (i.e., excluding the practice session) in the analyses reported in this paper. The time series of consecutive trial-wise stimuli, choices, RTs and pupil responses was necessary for the regression model of serial bias modulation. Observers were well-practiced in the task structure after the practice session. As a consequence, they made few blinks during the trial intervals (on average across observers, only 7.7% of trials contained more than 50% interpolated samples). The

percentage of interpolated trials did not correlate with the estimated effect of pupil responses on serial choice bias (r = -0.268, p = 0.175, Bf_{10} = 0.369).

Quantifying pupil timecourses and single-trial responses

To characterize the time-course of uncertainty encoding in the pupil response, we regressed across-trial evidence strength onto each sample of the baseline-corrected pupil signal, separately for correct and error trials (Figure 3b). The design matrix for this regression also included an intercept and three nuisance covariates: (i) log-transformed RTs, (ii) sample-by-sample horizontal gaze coordinates and (iii) sample-by sample vertical gaze coordinates. We tested the significance of this regression timecourse using cluster-based permutation statistics (Blair and Karniski 1993).

We took the mean baseline-corrected pupil signal during 250 ms before feedback delivery as our single-trial measure of pupil response. Because of the temporal low-pass characteristics of the sluggish peripheral pupil apparatus (Hoeks and Ellenbroek 1993), trial-to-trial variations in RT can cause trial-to-trial in pupil responses, even in the absence of amplitude variations in the underlying neural responses. To specifically isolate trial-to-trial variations in the amplitude (not duration) of the underlying neural responses, we removed components explained by RT via linear regression

$$\mathbf{y}' = \mathbf{y} - (\mathbf{y}^{\mathsf{T}}\mathbf{r})\mathbf{r} \tag{7}$$

where $\mathbf{y}$ was the original vector of pupil responses, $\mathbf{r}$ was the vector of the corresponding single-trial RTs (log-transformed and normalized to a unit vector), and T denoted matrix transpose. The residual $\mathbf{y}'$ thus reflected pupil responses, after removing variance explained by trial-by-trial RTs. This residual pupil response was used for all analyses reported in the main text.

Quantifying post-error slowing

We quantified post-error slowing, for tertiles of previous trial pupil responses, as described by Dutilh et al. 2012. Briefly, we selected those error trials that were both preceded and followed by a correct trial, and subtracted the pre-error RT from the associated post-error RT. This procedure ensured that estimates of post-error slowing could not be driven by error-unrelated, intrinsic fluctuations in RT over the course of a session. Before this subtraction, we removed trial-by-trial evidence strength from RTs using linear regression, to account for the large variations in RT with stronger sensory evidence (Figure 2d).

Quantifying the psychometric function

We modeled the psychometric function (Figure S4a) as follows. The probability of a particular response $r_t = 1$ on trial t was described as:

$$P(r_t = 1|\tilde{s_t}) = \gamma + (1 - \gamma - \lambda)g(\delta + \alpha\tilde{s_t}) \tag{8}$$

where λ and γ were the probabilities of stimulus-independent errors ('lapses'), $\tilde{s_t}$ was the signed stimulus intensity (here: signed sensory evidence as in Figure 2b), $g(x) = 1/(1+e^{-x})$ was the logistic function, α was perceptual sensitivity, and δ was a bias term. The free parameters γ, λ, α and δ were estimated by minimizing the negative log-likelihood of the data (using Matlab's *fminsearchbnd*). We constrained γ and λ to be identical, so as to estimate a single, choice-independent lapse rate.

For the quantification of serial choice bias (Figure S5), we binned the data by previous choices and by previous pupil responses or RT. For each of those subsets of trials, we fit the psychometric function (equation 8) to the choices on the subsequent trials. The resulting bias term α was transformed from log-odds into probability by $p = e^{\alpha}/(1+e^{\alpha})$. This quantified $P(r_t = 1)$ for ambiguous evidence (i.e., strength of zero). Collapsing these values across the two choice options (shown separately in Figure S5) yielded the pooled measure of choice repetition probability in Figure 4a,f.

Quantifying perceptual sensitivity using cumulative Weibull function fits

In Figure 3d, S1c and S3b, we fit a cumulative Weibull function to accuracy as a function of evidence strength. The probability of a correct response $c_t = 1$ on trial t was defined as:

$$P(c_t = 1|s_t) = 1 - (0.5 - \lambda) f\left((\frac{s_t}{\theta})^{\beta}\right) \tag{9}$$

where s_t was the absolute evidence strength, $f(x) = (1 - e^{-x})$ was the cumulative Weibull function, λ was the lapse rate, θ was the threshold indicating at which level of evidence strength an accuracy of ~80% is achieved, and β was the slope of the cumulative Weibull function. The free parameters θ, β and λ were estimated by minimizing the negative log-likelihood of the data (using Matlab's *fminsearchbnd*). Perceptual sensitivity was then defined as $1/\theta$.

Modeling the modulation of serial choice bias by uncertainty-dependent variables

We modeled the pupil- and RT-linked modulation of serial choice bias by extending an established regression approach (Fründ et al. 2014). The basic regression model extended the psychometric function model (equation 8) by means of a history-dependent bias term $\delta_{hist}(\mathbf{h}_t)$, which was a linear combination of previous stimuli and choices

$$P(r_t = 1|\tilde{s_t}\mathbf{h}_t) = \gamma + (1 - \gamma - \lambda) g(\delta(\mathbf{h}_t) + \alpha\tilde{s_t}) \tag{10}$$

with

$$\delta(\mathbf{h}_t) = \delta' + \delta_{hist}(\mathbf{h}_t) = \delta' + \sum_{k=1}^{K} \omega_k h_{kt} \tag{11}$$

where the bias term $\delta(\mathbf{h}_t)$ was the sum of the overall bias δ' (see equation 8) and the history bias $\delta_{hist}(\mathbf{h}_t) = \sum_{k=1}^{K} \omega_k h_{kt}$, where ω_k were the weights assigned to each previous stimulus or choice. We here modeled

$$\mathbf{h}_t = (r_{t-1},\ r_{t-2},\ r_{t-3},\ r_{t-4},\ r_{t-5},\ r_{t-6},\ r_{t-7},\ z_{t-1},\ z_{t-2},\ z_{t-3},\ z_{t-4},\ z_{t-5},\ z_{t-6},\ z_{t-7}) \tag{12}$$

as a concatenation of the last seven responses and stimuli (Fründ et al. 2014). This procedure allowed us to quantify the effect of past trials on current choice processes (Figure 5c). We convolved every set of seven past trials with three exponentially decaying basis functions (Fründ et al. 2014). Positive history weights ω_k indicated a tendency to repeat the previous choice, or to make a choice that matched the previous stimulus. Negative weights described a tendency to alternate the corresponding history feature.

To model the effect of pupil-linked uncertainty on history biases, we extended this model by adding a multiplicative interaction term $\sum_{k=1}^{K} \omega'_k h_{kt} p_{kt}$, which described the interaction of pupil responses with the choice and stimulus identities at the last seven lags:

$$P(r_t = 1 | \tilde{s_t}, \mathbf{h}_t, \mathbf{p}_t) = \gamma + (1 - \gamma - \lambda) g(\delta(\mathbf{h}_t, \mathbf{p}_t) + \alpha \tilde{s_t}) \tag{13}$$

with

$$\delta(\mathbf{h}_t, \mathbf{p}_t) = \delta' + \delta_{hist}(\mathbf{h}_t, \mathbf{p}_t) = \delta' + \sum_{k=1}^{K} \omega_k h_{kt} + \omega'_k h_{kt} p_{kt} + \omega''_k p_{kt} \tag{14}$$

where ω'_k were the history x pupil interaction weights, ω''_k were the pupil weights and

$$p_{kt} = (p_{t-1},\ p_{t-2},\ p_{t-3},\ p_{t-4},\ p_{t-5},\ p_{t-6},\ p_{t-7}\ )$$

was a concatenation of the last seven pupil responses. The term $\omega''_k p_{kt}$ acted as a nuisance covariate. To simultaneously model the effects of pupil responses and log-transformed RT, our model also included RT and history x RT terms, generated using the same procedure.

All parameters were fit using an expectation maximization algorithm. To assess whether individual observers were significantly influenced by their experimental history, we ran 1,000 iterations of permuting all trials, fitting the full model, and subsequently comparing the likelihood of the intact model to this null distribution (where permutation nullifies true history effects) (Fründ et al. 2014). Confidence intervals for individual regression weights were obtained from a bootstrapping procedure.

Serial bias and outcome-dependent choice strategies

The history weights for past stimuli and responses allowed us to characterize different decision strategies (Fründ et al. 2014) (Figure 5d). Positive weights associated with the previous choice, or the previous stimulus

category, indicate a tendency to repeat this previous choice, or to make a choice corresponding to the previous stimulus, respectively. Negative weights correspond to a tendency to alternate previous choice or stimulus. In the left and right triangle of this strategy space, the magnitude of the response weight is larger than the magnitude of the stimulus weight. Consequently, strategies are dominated by the previous choice and can be simply defined as choice alternation (left) or choice repetition (right).

In the upper and in the lower triangle, the magnitude of the stimulus weight is larger than the magnitude of the response weight, so strategies are dominated by the identity of the previous stimulus (which is only known to the observer as a function of their previous response and feedback). In the upper and lower triangle, strategies are thus defined by the sign of the stimulus weight. In the upper triangle stimulus weights are positive, indicating a tendency to repeat the previous stimulus. On a correct trial, previous choice and stimulus are equal and therefore, repeating the previous stimulus is equal to repeating the previous choice (a win-stay strategy). On errors, the previous choice is opposite to the previous stimulus and repeating the previous stimulus is equal to alternating the previous choice (lose-switch strategy). Conversely, in the lower triangle stimulus weights are negative, reflecting a tendency to alternate the previous stimulus. This implies a tendency to alternate the previous choice if the previous choice was correct (win-switch strategy) and a tendency to repeat the previous choice in case of a previous error (lose-stay strategy).

The weights for previous choices and stimuli can easily be combined to obtain weights reflecting a tendency to repeat previous correct or incorrect choices (Figure S6). Specifically, correct weights are defined by $\mathrm{choice} + \mathrm{stimulus}$, and error weights by $\mathrm{choice} - \mathrm{stimulus}$ (Fründ et al. 2014). The same holds for modulation weights. This transformation is identical to fitting a model with regressors for previous successes and failures (Busse et al. 2011; Abrahamyan et al. 2016).

Statistical tests

We used non-parametric permutation testing to test for the group-level significance of individually fitted parameter values (Figure 3 and Figure 5e,g). We randomly switched labels of individual observations either between two paired sets of values, between one set of values and zero, or between two unpaired groups. After repeating this procedure 10,000 times, and computing the difference between the two group means on each permutation, the p-value was the fraction of permutations that exceeded the observed difference between the means. All p-values reported were computed using two-sided tests.

In Figure 4, we split the data into tertiles of pupil response or RT, and computed next trial serial choice bias, signed choice bias, overall choice bias, perceptual sensitivity, lapse rate, RT and post-error slowing in each bin. We used a repeated-measures ANOVA to test for the main effect of bin on each dependent variable. We further used Bayes Factors (Bf), obtained from a Bayesian one-factor ANOVA (Rouder et al. 2012), to support conclusions about null effects observed. Bf_{10} quantifies the evidence in favour of the null or the alternative hypothesis, where $Bf_{10} < \frac{1}{3}$ or > 3 is taken to indicate substantial evidence for H_0 or H_1, respectively. $Bf_{10} = 1$ indicates inconclusive evidence. We similarly computed Bf_{10} for correlations, based

on the Pearson correlation coefficient (Wetzels and Wagenmakers 2012).

The p-value for the difference between the two correlation coefficients (choice weight by pupil modulation weight vs. choice weight by RT modulation weight), shown in Figure 5f, was obtained through permutation testing. To generate a null distribution of no difference, we randomly switched (or not, dependent on a simulated coin flip) each observer's RT and pupil modulation weights, after which we computed the between-subject correlation between choice weights and pupil modulation weights as well as between choice and RT modulation weights. Repeating this procedure 10,000 times generated a distribution of the difference in correlation, under the null hypothesis of no difference.

Data availability

All raw and processed data, as well as the code to reproduce all analyses and figures, are available at `http://dx.doi.org/10.6084/m9.figshare.4300043`.

Acknowledgements

We thank O'Jay Medina for assistance with data collection, all members of the Donnerlab for valuable discussions, and Konstantinos Tsetsos, Jan Willem de Gee, Niklas Wilming, Camile Correa, Florent Meyniel and Sander Nieuwenhuis for helpful comments on the manuscript. We acknowledge computing resources provided by NWO Physical Sciences. This research was supported by the German Academic Exchange Service (DAAD) and G.-A. Lienert Foundation (to A.E.U.) and the German Research Foundation (DFG), SFB 936/A7, SFB 936/Z1, DO 1240/2-1 and DO 1240/3-1, and European Union Seventh Framework Programme (FP7/2007-2013) under grant agreement no. 604102 (Human Brain Project) (to T.H.D.).

Supplementary Figures

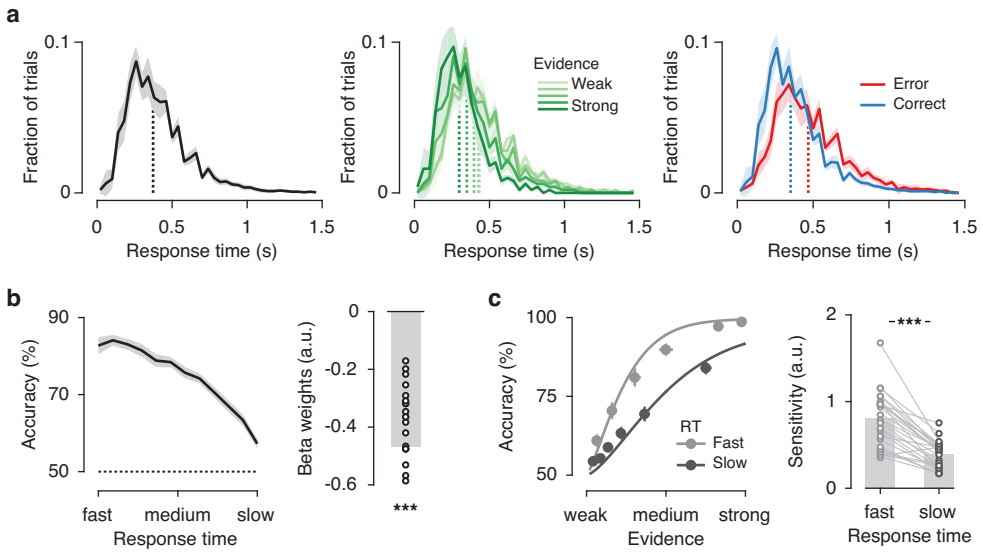

Figure S1. RTs scale with decision uncertainty. (**a**) RT distributions from stimulus offset, shown for all trials (left), split into five bins of evidence strength (middle), and separately for correct and error trials (right). For each observer, the number of trials was counted in each 40-ms wide bin from 0 to 1.5 seconds after stimulus offset, and normalized by the total number of trials. Shaded error bars indicate group median and inter-quartile range. Dotted line indicates group mean of individual RT medians. (**b**) RT predicted choice accuracy over a range from about 85% to about 60% correct, and not below chance level (50%). This relationship is consistent with decision uncertainty, but not error detection, which predicts accuracies of a range from 100% to 0% correct. Left: Accuracy for 12 bins of RT, shaded error bars indicate group mean ± s.e.m. Right: Individual logistic regression weights, using RT to predict single-trial accuracy. (**c**) Slow RTs reflected lower perceptual sensitivity. Left: Average cumulative Weibull psychometric function fits and data points (group mean ± s.e.m.), separately for the lowest and highest RT tertiles. Right: Individual perceptual sensitivity, separately for lowest and highest RT tertiles. In **b-c**, we z-scored and log-transformed RTs within each block and removed trial-to-trial variability shared with pupil responses via linear regression before computing statistics. *** $p < 0.001$, permutation test. (N=27, group mean ± s.e.m.)

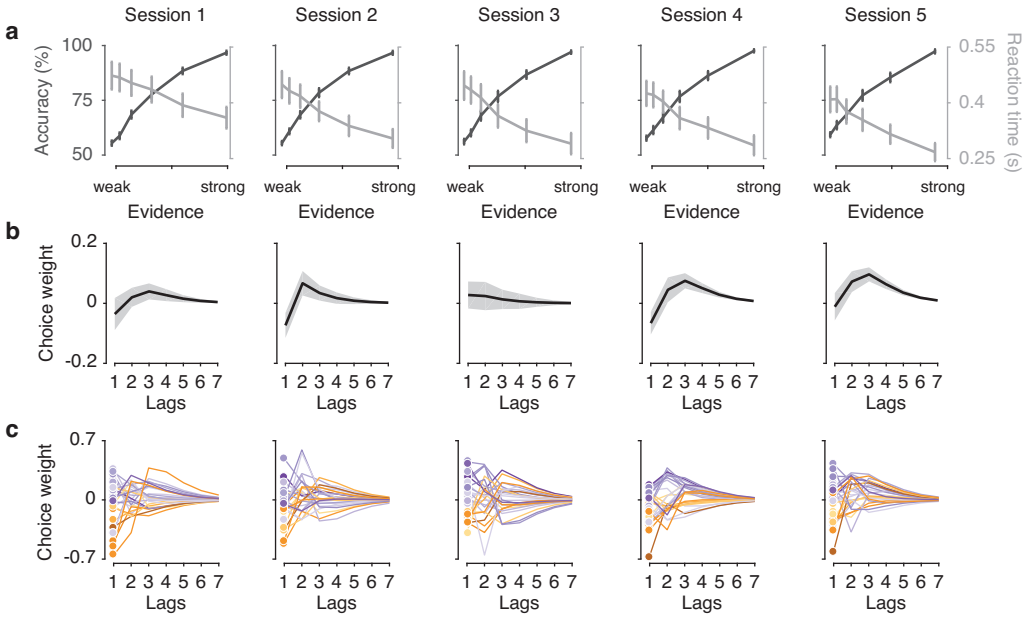

Figure S2. Behaviour over sessions. Data from each observer were collected over 5 main experimental sessions of 500 trials. Data from the practice session are not shown here. After discarding trials in which no response was recorded, each session contained an average of 498 trials (range 465-500). (**a**) Psychometric and chronometric functions, as in Figure 2d, separately for each session. (**b**) History kernels as in Figure 5c, separately for each session. (N=27, group mean ± s.e.m.) (**c**) Individual history kernels as in Figure 5c, separately for each session. Colors indicate the choice weight as derived from the model in Figure 5c-d, fit across all sessions combined. To complement these visual representations of behaviour over sessions, we computed repetition probability for three bins of pupil responses (Figure 4a), separately in each of the five sessions. Using a repeated measures ANOVA, we found no main effect of session ($F_{4,104}$ = 1.591, p = 0.182, Bf_{10} = 0.078) nor an interaction between session and pupil bin ($F_{8,208}$ = 1.333, p = 0.229, Bf_{10} = 0.023) on repetition probability. This analysis indicates that history biases do not detectably change over the course of learning, adding further evidence to the idea that serial choice biases are stable, individual traits.

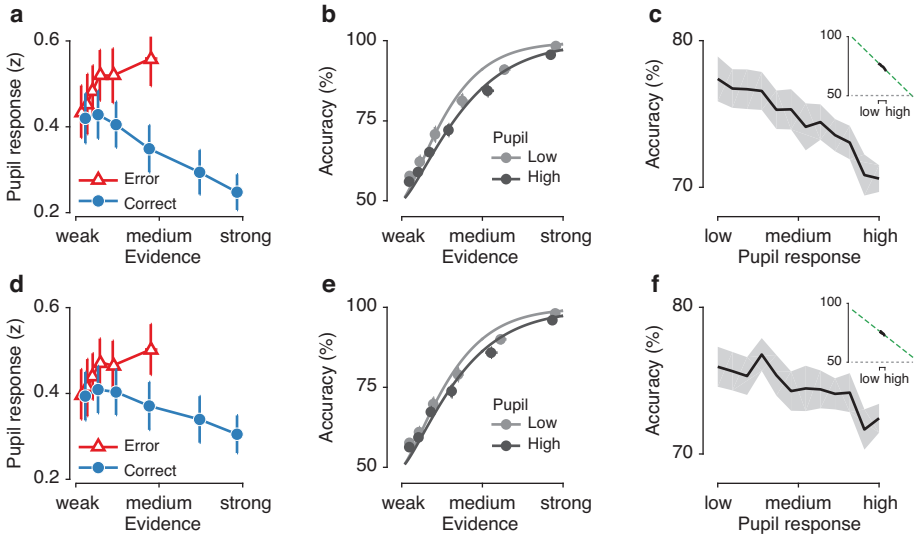

Figure S3. Pupil responses scale with decision uncertainty. Testing for all three signatures of decision uncertainty derived from the model in Figure 1. (**a**) Pupil responses scaled oppositely with evidence strength on correct and error trials. (**b**) High pupil responses reflected lower perceptual sensitivity. Average cumulative Weibull psychometric function fits (see Methods) and data points, separately for the lowest and highest tertiles of pupil responses. (**c**) Accuracy as a function of pupil responses (12 bins). Pupil responses predicted uncertainty over a range between 100% and 50% correct, but clearly not below 50% correct. This scaling is more consistent with decision uncertainty than with error awareness (which predicts accuracies down to 0%). Note that the analysis is limited by noise corrupting the single-trial pupil measurements. To address this issue, we fit a line to the data in **c**, extended its negative range to reach 100% accuracy, and then extended its positive range, with an equal distance. The result, shown in the inset, provided a rough estimate of the relationship expected, based on our result, if single-trial pupil-linked arousal could be measured without noise. Again, this analysis indicates that the scaling of pupil responses with accuracy is more consistent with decision uncertainty than with error awareness. (**d-e**) Same as **a-c**, after removing trial-by-trial fluctuations in log-transformed RT from the pupil signal using linear regression. The scaling of the pupil response with decision uncertainty was not inherited from the analogous scaling of RT. (N=27, group mean ± s.e.m.)

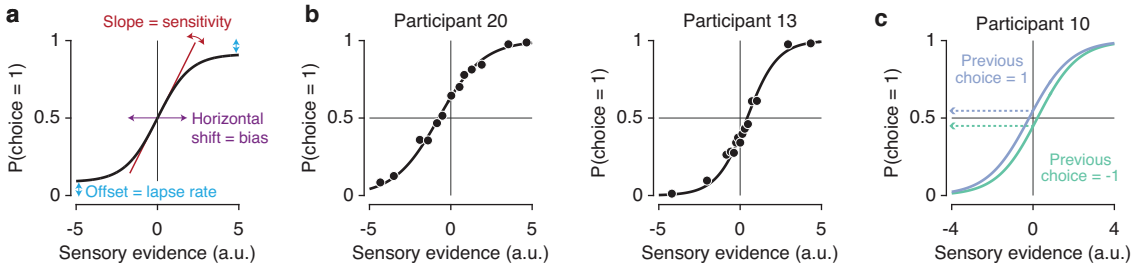

Figure S4. Quantifying choice bias using psychometric function fits. (**a**) A logistic psychometric function quantifies separate aspects of choice behaviour. The slope of the function indicates the observer's perceptual sensitivity. The intercept indicates a horizontal shift of the psychometric function, reflecting a bias towards a specific choice independent of the sensory evidence. The vertical offsets from the two asymptotes indicate the fraction of stimulus-independent errors ('lapses'). See also Methods. (**b**) Example psychometric functions with corresponding data points, for an example observer with a bias towards $\mathrm{choice}1$ (left) and an observer with a bias towards choice_{-1} (right). (**c**) History-dependent choice bias. Example observer with a tendency to repeat the previous choice.

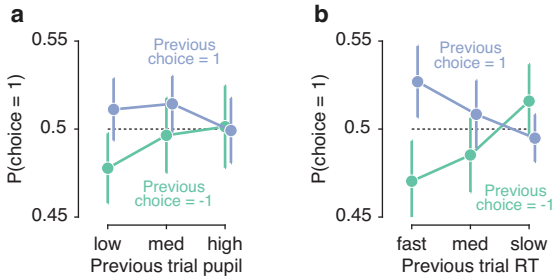

Figure S5. Pupil modulation of history-dependent choice bias. (**a**) Modulation of repetition probability by previous trial pupil response. $P(choice = 1)$ was computed from the intercept of the logistic function (see Methods), for tertiles of previous trial pupil responses. (**b**) as in a, but for tertiles of previous trial RT. The two choice identities were collapsed to obtain the measure of repetition probability in Figure 4a,f. (N=27, group mean ± s.e.m.)

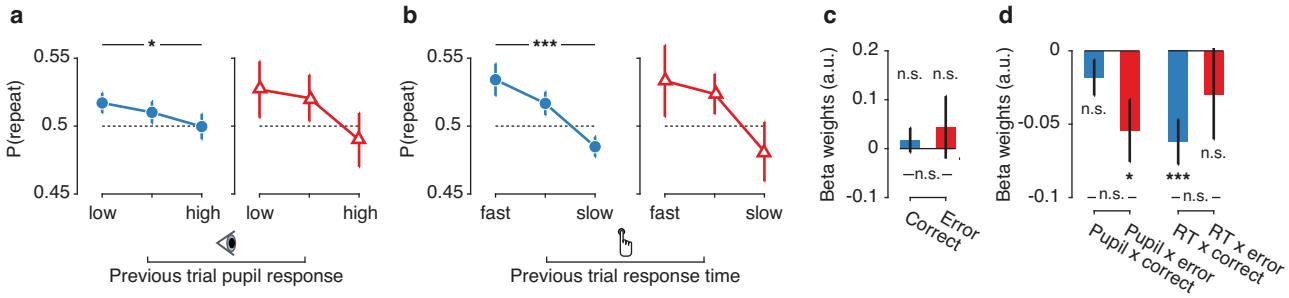

Figure S6. Pupil responses and RT modulate serial choice bias within categories of accuracy. (**a**) Repetition probability, for tertiles of previous trial pupil responses, separately for correct (left) and error (right) trials. (**b**) As in **a**, but for tertiles of previous trial RT. (**c**) Beta weights for repeating a previous correct vs. incorrect choice (see Methods). (**d**) Pupil- and RT modulation weights for repeating a previous correct vs. incorrect choice. Beta weights were obtained from the model show in Figure 5e-g, with pupil- and RT-linked modulatory terms included in the same regression model. Statistics indicate the main effect of a one-way ANOVA (**a, b**) or a permutation test (**c, d**). *** $p < 0.001$,* $p < 0.05$, n.s. $p > 0.05$. (N=27, group mean ± s.e.m.) These results indicate that the modulatory effect of pupil responses (and RT) on serial choice biases was not purely driven by higher pupil responses on error trials. Instead, serial choice bias was modulated by trial-to-trial fluctuations in pupil-linked arousal within categories of trial outcomes.

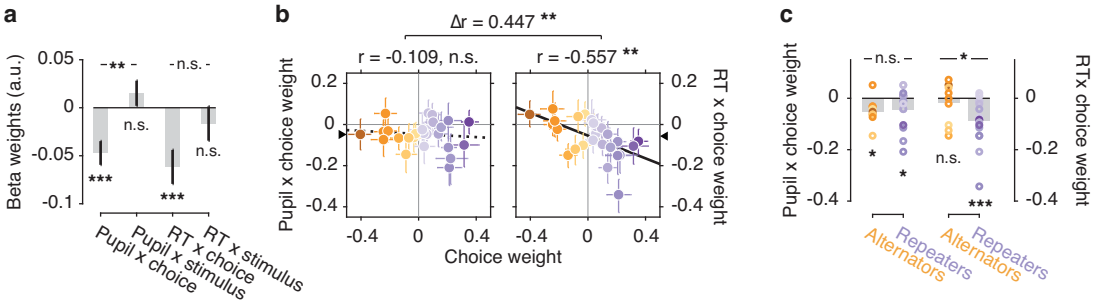

Figure S7. Modeling results do not depend on simultaneous fitting of both pupil and RT. Running two separate regression models, one including only pupil response and one only including RT as a modulatory variable, gives the same results as shown in Figure 5 (where the two were included in the regression model simultaneously). (**a-c**) as in Figure 5e-g, but with data obtained from two separate regression models.

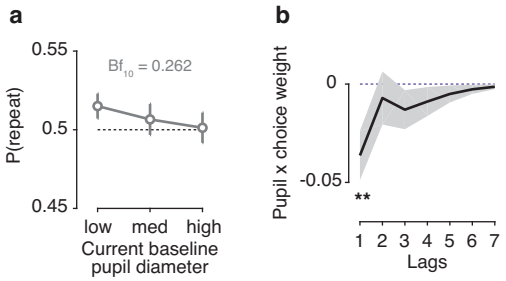

Figure S8. Predictive effect is specific for pupil response on the preceding trial. (**a**) Baseline pupil diameter on the current trial did not predict a modulation of serial choice bias. Repetition probability, for tertiles of current trial baseline pupil diameter (main effect of one-way repeated measured ANOVA, $F_{2,52}$ = 1.164, p = 0.320). (**b**) Pupil modulation of choice bias was only significant (** p < 0.01) across the group of observers at lag 1 (same data as Figure 5e), and did not reach significance beyond one trial in the past. This finding indicates that the modulation of choice biases by pupil responses was more short-lived than the overall serial choice biases shown in Figure 5c. (N=27, group mean ± s.e.m.)

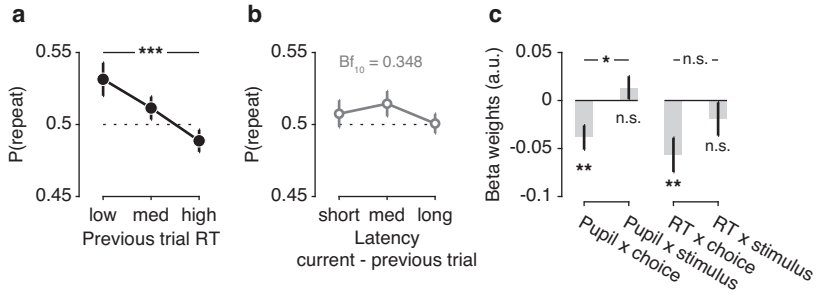

Figure S9. Serial choice biases are not explained by variations in interval timing. (**a**) To measure the passage of time between trials, we computed the latency between the onset of each test stimulus and the onset of the next trial?s test stimulus. These latencies correlated with RTs (mean Spearman's ± 0.296, range 0.086 to 0.726). Removing these trial-by-trial latencies from RT (using linear regression) did not abolish the effect of RTs on serial choice bias (main effect of RT bin, $F_{2,52}$ = 10.846, p < 0.001, Bf_{10}ha = 225.756). (**b**) Latencies did not predict a modulation of serial choice bias (main effect of latency bin, $F_{2,52}$ = 1.541, p = 0.224, Bf_{10} = 0.349). These results suggest that the uncertainty component of RTs, rather than the passage of time between trials, modulated serial choice bias. (**c**) We tested whether the modulation of serial bias by pupil response could be explained by trial-to-trial variations in the jittered interval between s1 and s2, or between button press and feedback delivery. When these random variations were long, they could cause larger pupil responses, irrespective of the amplitude of the underlying neural input, by driving the peripheral pupil apparatus for a longer duration. We removed these trial-to-trial interval durations from pupil responses using linear regression, and reran the analysis shown in Figure 5e. Although pupil responses were weakly correlated to the interval between s1 and s2 (mean Spearman's ρ -0.007, range -0.055 to 0.047, significant in 3 out of 27 observers) and the interval between button press and feedback (mean Spearman's ρ 0.056, range -0.025 to 0.290, significant in 13 out of 27 observers), removing this variance from trial-by-trial pupil responses did not change the predictive effect of pupil responses on serial choice bias. Statistics indicate the main effect of a one-way ANOVA (a, b) and permutation test (c). *** p < 0.001, ** p < 0.01, * p < 0.05, n.s. p < 0.05. (N=27, group mean ± s.e.m.)

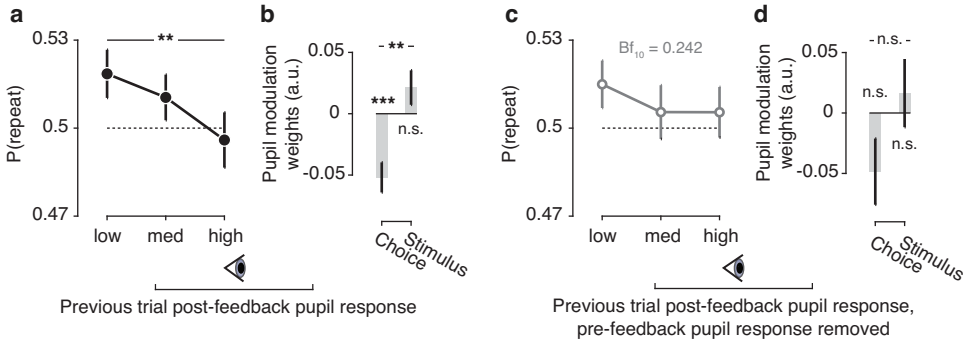

Figure S10. Serial choice biases are not explained by post-feedback pupil responses. To test whether serial choice biases were modulated by pupil responses to the feedback tone beyond pre-feedback uncertainty signaling, we computed post-feedback values as the mean pupil diameter 515-765 ms after feedback tone delivery. This window was defined as the peak of the grand average pupil response, and its length set equal to our pre-feedback window. (**a**) Serial choice bias for tertiles of previous trial post-feedback pupil responses (main effect of pupil bin, $F_{2,52}$ = 5.479, p = 0.007, Bf_{10} = 6.014). (**b**) Beta weights for the interaction between previous trial post-feedback pupil response and choice or stimulus, as in Figure 5e. (**c**) We removed the effect of single-trial pre-feedback from the post-feedback signal using linear regression. The residual reflected the effect of feedback on uncertainty scaling in the pupil, after taking into account the scaling already present before the feedback tone. Serial choice bias, for tertiles of residual pupil responses (main effect of pupil bin, $F_{2,52}$ = 1.063, p = 0.353) (d) Modulation weights for post-feedback pupil responses, with pre-feedback pupil responses added as a covariate in the same regression model. The information about serial biases was already contained in the pupil signal before feedback delivery. Statistics indicate the main effect of a one-way ANOVA (**a, c**) and permutation test (**b, d**) . *** p < 0.001, ** p < 0.01, n.s. p > 0.05. (N=27, group mean ± s.e.m.)

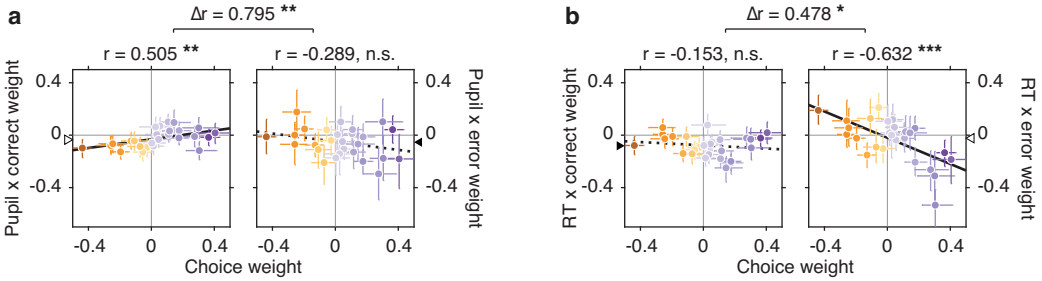

Figure S11. Differential gating of individual choice modulation by trial outcome. Pupil-and RT-linked modulations of serial choice bias were differentially gated by trial outcome. We computed correct and error modulation weights from choice and stimulus modulation weights (see Methods). (**a**) Correlation between choice weights and pupil modulation weights, separately for correct and incorrect choices. (**b**) Correlation between choice weights and RT modulation weights, separately for correct and incorrect choices. Colors indicate the choice weight as derived from the basic model in Figure 5c. Error bars indicate a 68% confidence interval obtained from a bootstrap. Triangles mark the intercept of a linear regression line; filled triangles indicate a group-level effect different from zero (as in Figure S6d). *** p < 0.001, ** p < 0.01, * p < 0.05, n.s. p > 0.05. Figure 5f shows that RT reduced observers' intrinsic serial biases while pupil responses generally promoted choice alternation. These results further dissociate these modulatory effects, in showing that they were 'gated' by trial outcome in distinct ways: Large pupil-linked arousal pushed observers to increase their intrinsic serial bias after correct trials, as indicated by the positive correlation in a. After error trials, on the other hand, a correlation of the opposite sign was observed indicating that across trial outcomes, these two effects nullified and lead to an overall boost in alternation. This stood in sharp contrast to the group-level effect of RT, which predicted a reduction in intrinsic serial bias across the group. This effect was strongly present after error trials (**b**), suggesting an adaptive control mechanism could be at work only after negative feedback is received. After correct trials, high RTs indicated a slight reduction in bias, but this negative correlation was not significant across the group.

5 | Bibliography

Abrahamyan A et al. (2016). Adaptable History Biases in Human Perceptual Decisions. *Proceedings of the National Academy of Sciences* 113(25):E3548–E3557.

Adelson EH, Bergen JR (1985). Spatiotemporal Energy Models for the Perception of Motion. *Journal of the Optical Society of America A* 2(2):284–299.

Akaishi R, Umeda K, Nagase A, Sakai K (2014). Autonomous Mechanism of Internal Choice Estimate Underlies Decision Inertia. *Neuron* 81(1):195–206.

Allefeld C et al. (2013). Sequential Dependencies between Trials in Free Choice Tasks. *arXiv* 1311:0753.

Ashby FG (1983). A Biased Random Walk Model for Two Choice Reaction Times. *Journal of Mathematical Psychology* 27(3):277–297.

Aston-Jones G, Cohen JD (2005). An Integrative Theory of Locus Coeruleus-Norepinephrine Function: Adaptive Gain and Optimal Performance. *Annual Review of Neuroscience* 28:403–450.

Baron-Cohen S et al. (2001). The Autism-Spectrum Quotient (AQ): Evidence from Asperger Syndrome/High-Functioning Autism, Males and Females, Scientists and Mathematicians. *Journal of Autism and Developmental Disorders* 31(1):5–17.

Benjamini Y, Hochberg Y (1995). Controlling the False Discovery Rate: A Practical and Powerful Approach to Multiple Testing. *Journal of the Royal Statistical Society. Series B (Methodological)*:289–300.

Bennur S, Gold JI (2011). Distinct Representations of a Perceptual Decision and the Associated Oculomotor Plan in the Monkey Lateral Intraparietal Area. *Journal of Neuroscience* 31(3):913–921.

Berens P (2009). CircStat: A MATLAB Toolbox for Circular Statistics. *Journal of Statistical Software* 31(10):1–21.

Bitzer S, Bruineberg J, Kiebel SJ (2015). A Bayesian Attractor Model for Perceptual Decision Making. *PLoS Computational Biology* 11(8):e1004442.

Blair RC, Karniski W (1993). An Alternative Method for Significance Testing of Waveform Difference Potentials. *Psychophysiology* 30(5):518–524.

Bode S et al. (2012). Predicting Perceptual Decision Biases from Early Brain Activity. *Journal of Neuroscience* 32(36):12488–12498.

Bogacz R, Cohen JD (2004). Parameterization of Connectionist Models. *Behavior Research Methods, Instruments, & Computers* 36(4):732–741.

Bogacz R, Wagenmakers EJ, Forstmann BU, Nieuwenhuis S (2010). The Neural Basis of the Speed–Accuracy Tradeoff. *Trends in Neurosciences* 33(1):10–16.

Bogacz R et al. (2006). The Physics of Optimal Decision Making: A Formal Analysis of Models of Performance in Two-Alternative Forced-Choice Tasks. *Psychological Review* 113(4):700–765.

Bonaiuto JJ, Berker A de, Bestmann S (2016). Response Repetition Biases in Human Perceptual Decisions Are Explained by Activity Decay in Competitive Attractor Models. *eLife* 5:e20047.

Botvinick MM et al. (2001). Conflict Monitoring and Cognitive Control. *Psychological Review* 108(3):624.

Bouret S, Sara SJ (2005). Network Reset: A Simplified Overarching Theory of Locus Coeruleus Noradrenaline Function. *Trends in Neurosciences* 28(11):574–582.

Braun A, Urai AE, Donner TH (2017). Confidence-Dependent Accumulation of Past Decision Variables Biases Perceptual Choice. *bioRxiv* 172049.

Britten KH et al. (1996). A Relationship between Behavioral Choice and the Visual Responses of

Neurons in Macaque MT. *Visual Neuroscience* 13(01):87–100.

Brody CD, Hanks TD (2016). Neural Underpinnings of the Evidence Accumulator. *Current Opinion in Neurobiology* 37:149–157.

Bronfman ZZ et al. (2015). Decisions Reduce Sensitivity to Subsequent Information. *Proceedings of the Royal Society B: Biological Sciences* 282(1810).

Brooks JL (2012). Counterbalancing for Serial Order Carryover Effects in Experimental Condition Orders. *Psychological Methods* 17(4):600–614.

Buffalo EA et al. (2010). A Backward Progression of Attentional Effects in the Ventral Stream. *Proceedings of the National Academy of Sciences* 107(1):361–365.

Busse L et al. (2011). The Detection of Visual Contrast in the Behaving Mouse. *Journal of Neuroscience* 31(31):11351–11361.

Carpenter RHS, Williams MLL (1995). Neural Computation of Log Likelihood in Control of Saccadic Eye Movements. *Nature* 377(6544):59–62.

Carver CS, White TL (1994). Behavioral Inhibition, Behavioral Activation, and Affective Responses to Impending Reward and Punishment: The BIS/BAS Scales. *Journal of Personality and Social Psychology* 67(2):319.

Cavanagh JF, Masters SE, Bath K, Frank MJ (2014). Conflict Acts as an Implicit Cost in Reinforcement Learning. *Nature Communications* 5:5394.

Chamberlain SR et al. (2009). Atomoxetine Modulates Right Inferior Frontal Activation During Inhibitory Control: A Pharmacological Functional Magnetic Resonance Imaging Study. *Biological Psychiatry* 65(7):550–555.

Chen MK, Risen JL (2010). How Choice Affects and Reflects Preferences: Revisiting the Free-Choice Paradigm. *Journal of Personality and Social Psychology* 99(4):573–594.

Cho RY et al. (2002). Mechanisms Underlying Dependencies of Performance on Stimulus History in a Two-Alternative Forced-Choice Task. *Cognitive, Affective, & Behavioral Neuroscience* 2(4):283–299.

Crapse TB, Basso MA (2015). Insights into Decision Making Using Choice Probability. *Journal of Neurophysiology* 114(6):3039–3049.

Cross DV (1973). Sequential Dependencies and Regression in Psychophysical Judgments. *Perception & Psychophysics* 14(3):547–552.

Dayan P, Kakade S, Montague PR (2000). Learning and Selective Attention. *Nature Neuroscience* 3:1218–1223.

Dayan P, Yu AJ (2006). Phasic Norepinephrine: A Neural Interrupt Signal for Unexpected Events. *Network: Computation in Neural Systems* 17(4):335–350.

de Berker AO et al. (2016). Computations of Uncertainty Mediate Acute Stress Responses in Humans. *Nature Communications* 7:10996.

de Gee JW, Knapen T, Donner TH (2014). Decision-Related Pupil Dilation Reflects Upcoming Choice and Individual Bias. *Proceedings of the National Academy of Sciences* 111(5):E618–E625.

de Gee JW et al. (2017). Dynamic Modulation of Decision Biases by Brainstem Arousal Systems. *eLife* 6:e23232.

de Lafuente V, Jazayeri M, Shadlen MN (2015). Representation of Accumulating Evidence for a Decision in Two Parietal Areas. *Journal of Neuroscience* 35(10):4306–4318.

de Lange FP, Rahnev DA, Donner TH, Lau H (2013). Prestimulus Oscillatory Activity over Motor Cortex Reflects Perceptual Expectations. *Journal of Neuroscience* 33(4):1400–1410.

Desimone R, Duncan J (1995). Neural Mechanisms of Selective Visual Attention. *Annual Review of Neuroscience* 18(1):193–222.

Donders FC (1868). Over de snelheid van psychische processen. *Onderzoekingen gedaan in het Physiologisch Laboratorium der Utrechtsche Hoogeschool (1968–1869)* 2:92–120.

Donner TH, Sagi D, Bonneh YS, Heeger DJ (2013). Retinotopic Patterns of Correlated Fluctuations in Visual Cortex Reflect the Dynamics of Spontaneous Perceptual Suppression. *Journal of Neuroscience* 33(5):2188–2198.

Donner TH, Siegel M, Fries P, Engel AK (2009). Buildup of Choice-Predictive Activity in Human Motor Cortex during Perceptual Decision Making. *Current Biology* 19(18):1581–1585.

Dutilh G et al. (2012). How to Measure Post-Error Slowing: A Confound and a Simple Solution. *Journal of Mathematical Psychology* 56(3):208–216.

Ebitz RB, Platt M (2015). Neuronal Activity in Primate Dorsal Anterior Cingulate Cortex Signals Task Conflict and Predicts Adjustments in Pupil-Linked Arousal. *Neuron* 85(3):628–640.

Edwards W (1965). Optimal Strategies for Seeking Information: Models for Statistics, Choice Reaction Times, and Human Information Processing. *Journal of Mathematical Psychology* 2(2):312–329.

Efron B, Tibshirani R (1986). Bootstrap Methods for Standard Errors, Confidence Intervals, and Other Measures of Statistical Accuracy. *Statistical Science* 1(1):54–75.

Einhäuser W, Stout J, Koch C, Carter O (2008). Pupil Dilation Reflects Perceptual Selection and Predicts Subsequent Stability in Perceptual Rivalry. *Proceedings of the National Academy of Sciences* 105(5):1704–1709.

Eldar E, Cohen JD, Niv Y (2013). The Effects of Neural Gain on Attention and Learning. *Nature Neuroscience* 16(8):1146–1153.

Fechner GT (1860). *Elemente der psychophysik*. Leipzig : Breitkopf und Härtel.

Fernberger SW (1920). Interdependence of Judgments within the Series for the Method of Constant Stimuli. *Journal of Experimental Psychology* 3(2):126.

Festinger L (1957). *A Theory of Cognitive Dissonance*. Stanford University Press.

Filimon F et al. (2013). How Embodied Is Perceptual Decision Making? Evidence for Separate Processing of Perceptual and Motor Decisions. *Journal of Neuroscience* 33(5):2121–2136.

Fischer J, Whitney D (2014). Serial Dependence in Visual Perception. *Nature Neuroscience* 17(5):738–743.

Freitag CM et al. (2007). Evaluation Der Deutschen Version Des Autismus-Spektrum-Quotienten (AQ) - Die Kurzversion AQ-K. *Zeitschrift für Klinische Psychologie und Psychotherapie* 36(4):280–289.

Fritsche M, Mostert P, de Lange FP (2017). Opposite Effects of Recent History on Perception and Decision. *Current Biology* 27(4):590–595.

Fründ I, Wichmann FA, Macke JH (2014). Quantifying the Effect of Intertrial Dependence on Perceptual Decisions. *Journal of Vision* 14(7):9–9.

Gallitto E, Leth-Steensen C (2015). Autistic Traits and Adult Attachment Styles. *Personality and Individual Differences* 79:63–67.

Gao J, Tortell R, McClelland JL (2011). Dynamic Integration of Reward and Stimulus Information in Perceptual Decision-Making. *PLoS ONE* 6(3):e16749.

Gao J et al. (2009). Sequential Effects in Two-Choice Reaction Time Tasks: Decomposition and Synthesis of Mechanisms. *Neural Computation* 21(9):2407–2436.

Gilbert CD, Li W (2013). Top-down Influences on Visual Processing. *Nature Reviews Neuroscience* 14(5):350–363.

Glaze CM, Kable JW, Gold JI (2015). Normative Evidence Accumulation in Unpredictable Environments. *eLife* 4:e08825.

Glimcher PW (2005). Indeterminacy in Brain and Behavior. *Annual Review of Psychology* 56(1):25–56.

Glimcher PW (2011). Understanding Dopamine and Reinforcement Learning: The Dopamine Reward Prediction Error Hypothesis. *Proceedings of the National Academy of Sciences* 108:15647–15654.

Gold JI, Law CT, Connolly P, Bennur S (2008). The Relative Influences of Priors and Sensory Evidence on an Oculomotor Decision Variable During Perceptual Learning. *Journal of Neurophysiology* 100(5):2653–2668.

Gold JI, Shadlen MN (2002). Banburismus and the Brain. *Neuron* 36(2):299–308.

Gold JI, Shadlen MN (2007). The Neural Basis of Decision Making. *Annual Review of Neuroscience* 30(1):535–574.

Gold JI, Stocker AA (2017). Visual Decision-Making in an Uncertain and Dynamic World. *Annual Review of Vision Science* 3:227–250.

Goldfarb S et al. (2012). Can Post-Error Dynamics Explain Sequential Reaction Time Patterns? *Cognitive Science* 3:213.

Good IJ (1979). Studies in the History of Probability and Statistics. XXXVII A. M. Turing's Statistical Work in World War II. *Biometrika* 66(2):393–396.

Goris RLT et al. (2017). Dissociation of Choice Formation and Choice-Correlated Activity in Macaque Visual Cortex. *Journal of Neuroscience* 37(20):5195–5203.

Gottlieb J (2012). Attention, Learning, and the Value of Information. *Neuron* 76(2):281–295.

Green DM, Swets JA (1966). *Signal Detection Theory and Psychophysics*. John Wiley and Sons.

Gross J et al. (2001). Dynamic Imaging of Coherent Sources: Studying Neural Interactions in the Human

Brain. *Proceedings of the National Academy of Sciences* 98(2):694–699.

Harris KD, Thiele A (2011). Cortical State and Attention. *Nature Reviews Neuroscience* 12:509–523.

Hebart MN, Donner TH, Haynes JD (2012). Human Visual and Parietal Cortex Encode Visual Choices Independent of Motor Plans. *NeuroImage* 63(3):1393–1403.

Hebart MN, Schriever Y, Donner TH, Haynes JD (2016). The Relationship between Perceptual Decision Variables and Confidence in the Human Brain. *Cerebral Cortex* 26(1):118–130.

Hebb DO (1949). *The Organization of Behavior: A Neuropsychological Theory*. New York: Wiley.

Hipp JF, Siegel M (2013). Dissociating Neuronal Gamma-Band Activity from Cranial and Ocular Muscle Activity in EEG. *Frontiers in Human Neuroscience* 7.

Hoeks B, Ellenbroek BA (1993). A Neural Basis for a Quantitative Pupillary Model. *Journal of Psychophysiology* 7:315–324.

Holmes CJ et al. (1998). Enhancement of MR Images Using Registration for Signal Averaging. *Journal of Computer Assisted Tomography* 22(2):324–333.

Hunt LT, Hayden BY (2017). A Distributed, Hierarchical and Recurrent Framework for Reward-Based Choice. *Nature Reviews Neuroscience* 18(3):172–182.

Insabato A, Pannunzi M, Rolls ET, Deco G (2010). Confidence-Related Decision Making. *Journal of Neurophysiology* 104(1):539–547.

Izuma K, Murayama K (2013). Choice-Induced Preference Change in the Free-Choice Paradigm: A Critical Methodological Review. *Frontiers in Psychology* 4:41.

Jazayeri M, Movshon JA (2006). Optimal Representation of Sensory Information by Neural Populations. *Nature Neuroscience* 9(5):690–696.

Jazayeri M, Movshon JA (2007). A New Perceptual Illusion Reveals Mechanisms of Sensory Decoding. *Nature* 446(7138):912–915.

Jones AD et al. (2002). A Computational Model of Anterior Cingulate Function in Speeded Response Tasks: Effects of Frequency, Sequence, and Conflict. *Cognitive, Affective & Behavioral Neuroscience* 2(4):300–317.

Joshi S, Li Y, Kalwani RM, Gold JI (2016). Relationships between Pupil Diameter and Neuronal Activity in the Locus Coeruleus, Colliculi, and Cingulate Cortex. *Neuron* 89(1):221–234.

Karlsson MP, Tervo DGR, Karpova AY (2012). Network Resets in Medial Prefrontal Cortex Mark the Onset of Behavioral Uncertainty. *Science* 338(6103):135–139.

Kass RE, Raftery AE (1995). Bayes Factors. *Journal of the American Statistical Association* 90(430):773–795.

Katahira K (2016). How Hierarchical Models Improve Point Estimates of Model Parameters at the Individual Level. *Journal of Mathematical Psychology* 73:37–58.

Katz LN, Yates JL, Pillow JW, Huk AC (2016). Dissociated Functional Significance of Decision-Related Activity in the Primate Dorsal Stream. *Nature* 535(7611):285–288.

Kelly SP, O'Connell RG (2013). Internal and External Influences on the Rate of Sensory Evidence Accumulation in the Human Brain. *Journal of Neuroscience* 33(50):19434–19441.

Kepecs A, Mainen ZF (2012). A Computational Framework for the Study of Confidence in Humans and Animals. *Philosophical Transactions of the Royal Society B: Biological Sciences* 367(1594):1322–1337.

Kepecs A, Uchida N, Zariwala HA, Mainen ZF (2008). Neural Correlates, Computation and Behavioural Impact of Decision Confidence. *Nature* 455(7210):227–231.

Kiani R, Hanks TD, Shadlen MN (2008). Bounded Integration in Parietal Cortex Underlies Decisions Even When Viewing Duration Is Dictated by the Environment. *Journal of Neuroscience* 28(12):3017–3029.

Kiani R, Shadlen MN (2009). Representation of Confidence Associated with a Decision by Neurons in the Parietal Cortex. *Science* 324(5928):759–764.

Kim TD, Kabir M, Gold JI (2017). Coupled Decision Processes Update and Maintain Saccadic Priors in a Dynamic Environment. *Journal of Neuroscience* 37(13):3632–3645.

Kira S, Yang T, Shadlen MN (2015). A Neural Implementation of Wald's Sequential Probability Ratio Test. *Neuron* 85(4):861–873.

Kiyonaga A, Scimeca JM, Bliss DP, Whitney D (2017). Serial Dependence across Perception, Attention, and Memory. *Trends in Cognitive Sciences* 21(7):493–497.

Klein SA (2001). Measuring, Estimating, and Understanding the Psychometric Function: A

Commentary. *Perception & Psychophysics* 63(8):1421–1455.

Kleiner M et al. (2007). What's New in Psychtoolbox-3. *Perception* 36(14):1–1.

Kloosterman NA et al. (2015a). Pupil Size Tracks Perceptual Content and Surprise. *European Journal of Neuroscience* 41(8):1068–1078.

Kloosterman NA et al. (2015b). Top-down Modulation in Human Visual Cortex Predicts the Stability of a Perceptual Illusion. *Journal of Neurophysiology* 113(4):1063–1076.

Knapen T et al. (2016). Cognitive and Ocular Factors Jointly Determine Pupil Responses under Equiluminance. *PLoS ONE* 11(5):e0155574.

Kohn A (2007). Visual Adaptation: Physiology, Mechanisms, and Functional Benefits. *Journal of Neurophysiology* 97(5):3155–3164.

Kok P, Brouwer GJ, van Gerven MAJ, de Lange FP (2013). Prior Expectations Bias Sensory Representations in Visual Cortex. *Journal of Neuroscience* 33(41):16275–16284.

Kok P, Mostert P, de Lange FP (2017). Prior Expectations Induce Prestimulus Sensory Templates. *Proceedings of the National Academy of Sciences* 114(39):10473–10478.

Komura Y et al. (2013). Responses of Pulvinar Neurons Reflect a Subject's Confidence in Visual Categorization. *Nature Neuroscience* 16(6):749–755.

Krishnamurthy K, Nassar MR, Sarode S, Gold JI (2017). Arousal-Related Adjustments of Perceptual Biases Optimize Perception in Dynamic Environments. *Nature Human Behaviour* 1:0107.

Kruschke JK (2013). Bayesian Estimation Supersedes the t Test. *Journal of Experimental Psychology: General* 142(2):573.

Lak A et al. (2014). Orbitofrontal Cortex Is Required for Optimal Waiting Based on Decision Confidence. *Neuron* 84(1):190–201.

Laming D (1968). *Information Theory of Choice-Reaction Times*. London: Academic Press Inc.

Latimer KW et al. (2015). Single-Trial Spike Trains in Parietal Cortex Reveal Discrete Steps during Decision-Making. *Science* 349(6244):184–187.

Lee SH, Dan Y (2012). Neuromodulation of Brain States. *Neuron* 76(1):209–222.

Leite FP, Ratcliff R (2011). What Cognitive Processes Drive Response Biases? A Diffusion Model Analysis. *Judgment & Decision Making* 6(7):651–687.

Lempert KM, Chen YL, Fleming SM (2015). Relating Pupil Dilation and Metacognitive Confidence during Auditory Decision-Making. *PLoS ONE* 10(5):e0126588.

Leopold DA, Wilke M, Maier A, Logothetis NK (2002). Stable Perception of Visually Ambiguous Patterns. *Nature Neuroscience* 5(6):605.

Licata AM et al. (2017). Posterior Parietal Cortex Guides Visual Decisions in Rats. *Journal of Neuroscience* 37(19):4954–4966.

Link SW, Heath RA (1975). A Sequential Theory of Psychological Discrimination. *Psychometrika* 40(1):77–105.

Liu F, Wang XJ (2008). A Common Cortical Circuit Mechanism for Perceptual Categorical Discrimination and Veridical Judgment. *PLoS Computational Biology* 4(12):e1000253.

Logothetis NK, Schall JD (1989). Neuronal Correlates of Subjective Visual Perception. *Science* 245(4919):761–763.

Luce RD (1986). *Response Times: Their Role in Inferring Elementary Mental Organization*. Oxford University Press.

Luu L, Stocker AA (2016). Choice-Induced Biases in Perception. *bioRxiv* 043224.

Ma WJ, Jazayeri M (2014). Neural Coding of Uncertainty and Probability. *Annual Review of Neuroscience* 37(1):205–220.

Macmillan NA, Creelman CD (2004). *Detection Theory: A User's Guide*. Mahwah, NJ: Lawrence Erlbaum Associates.

Marder E (2012). Neuromodulation of Neuronal Circuits: Back to the Future. *Neuron* 76(1):1–11.

Maris E, Oostenveld R (2007). Nonparametric Statistical Testing of EEG- and MEG-Data. *Journal of Neuroscience Methods* 164(1):177–190.

McDougal DH, Gamlin PDR (2008). Pupillary Control Pathways. *The Senses: A Comprehensive Reference*. Ed. by Albright TD et al. New York: Academic Press, pp. 521–536.

McGinley MJ, David S, McCormick D (2015a). Cortical Membrane Potential Signature of Optimal States for Sensory Signal Detection. *Neuron* 87(1):179–192.

McGinley MJ et al. (2015b). Waking State: Rapid Variations Modulate Neural and Behavioral Responses. *Neuron* 87(6):1143–1161.

Meindertsma T et al. (2017). Multiple Transient Signals in Human Visual Cortex Associated with an Elementary Decision. *Journal of Neuroscience*:3835–16.

Meyer TJ, Miller ML, Metzger RL, Borkovec TD (1990). Development and Validation of the Penn State Worry Questionnaire. *Behaviour Research and Therapy* 28(6):487–495.

Meyniel F, Maheu M, Dehaene S (2016). Human Inferences about Sequences: A Minimal Transition Probability Model. *PLoS Computational Biology* 12(12):e1005260.

Meyniel F, Schlunegger D, Dehaene S (2015). The Sense of Confidence during Probabilistic Learning: A Normative Account. *PLoS Computational Biology* 11(6):e1004305.

Miller EK, Cohen JD (2001). An Integrative Theory of Prefrontal Cortex Function. *Annual Review of Neuroscience* 24(1):167–202.

Mitra PP, Pesaran B (1999). Analysis of Dynamic Brain Imaging Data. *Biophysical Journal* 76(2):691–708.

Morcos AS, Harvey CD (2016). History-Dependent Variability in Population Dynamics during Evidence Accumulation in Cortex. *Nature Neuroscience* 19(12):1672–1681.

Mulder MJ et al. (2012). Bias in the Brain: A Diffusion Model Analysis of Prior Probability and Potential Payoff. *Journal of Neuroscience* 32(7):2335–2343.

Muris P, Merckelbach H, Wessel I, van de Ven M (1999). Psychopathological Correlates of Self-Reported Behavioural Inhibition in Normal Children. *Behaviour Research and Therapy* 37(6):575–584.

Murphy PR, Boonstra E, Nieuwenhuis S (2016a). Global Gain Modulation Generates Time-Dependent Urgency during Perceptual Choice in Humans. *Nature Communications* 7:13526.

Murphy PR, van Moort ML, Nieuwenhuis S (2016b). The Pupillary Orienting Response Predicts Adaptive Behavioral Adjustment after Errors. *PLoS ONE* 11(3):e0151763.

Murphy PR et al. (2014). Pupil Diameter Covaries with BOLD Activity in Human Locus Coeruleus: Pupil Diameter and Locus Coeruleus Activity. *Human Brain Mapping* 35(8):4140–4154.

Nassar MR et al. (2012). Rational Regulation of Learning Dynamics by Pupil-Linked Arousal Systems. *Nature Neuroscience* 15(7):1040–1046.

Newsome WT, Britten KH, Movshon JA (1989). Neuronal Correlates of a Perceptual Decision. *Nature* 341(6237):52–54.

Nichols MJ, Newsome WT (2002). Middle Temporal Visual Area Microstimulation Influences Veridical Judgments of Motion Direction. *Journal of Neuroscience* 22(21):9530–9540.

Nickerson RS (1998). Confirmation Bias: A Ubiquitous Phenomenon in Many Guises. *Review of General Psychology* 2(2):175.

Nienborg H, Cumming BG (2006). Macaque V2 Neurons, But Not V1 Neurons, Show Choice-Related Activity. *Journal of Neuroscience* 26(37):9567–9578.

Nienborg H, Cumming BG (2009). Decision-Related Activity in Sensory Neurons Reflects More than a Neuron's Causal Effect. *Nature* 459(7243):89–92.

Nienborg H, Roelfsema PR (2015). Belief States as a Framework to Explain Extra-Retinal Influences in Visual Cortex. *Current Opinion in Neurobiology* 32:45–52.

Nolte G (2003). The Magnetic Lead Field Theorem in the Quasi-Static Approximation and Its Use for Magnetoencephalography Forward Calculation in Realistic Volume Conductors. *Physics in Medicine and Biology* 48(22):3637–3652.

O'Connell RG, Dockree PM, Kelly SP (2012). A Supramodal Accumulation-to-Bound Signal That Determines Perceptual Decisions in Humans. *Nature Neuroscience* 15(12):1729–1735.

Odoemene O, Nguyen H, Churchland AK (2017). Visual Evidence Accumulation Behavior in Unrestrained Mice. *bioRxiv* 195792.

Oostenveld R, Fries P, Maris E, Schoffelen JM (2011). FieldTrip: Open Source Software for Advanced Analysis of MEG, EEG, and Invasive Electrophysiological Data. *Computational Intelligence and Neuroscience* (156869).

O'Reilly JX et al. (2013). Dissociable Effects of Surprise and Model Update in Parietal and Anterior Cingulate Cortex. *Proceedings of the National Academy of Sciences* 110(38):E3660–E3669.

Ossmy O et al. (2013). The Timescale of Perceptual Evidence Integration Can Be Adapted to the Environment. *Current Biology* 23(11):981–986.

Padoa-Schioppa C (2013). Neuronal Origins of Choice Variability in Economic Decisions. *Neuron* 80(5):1322–1336.

Pape AA, Siegel M (2016). Motor Cortex Activity Predicts Response Alternation during Sensorimotor Decisions. *Nature Communications* 7:13098.

Park-Wyllie LY et al. (2009). Cholinesterase Inhibitors and Hospitalization for Bradycardia: A Population-Based Study. *PLOS Medicine* 6(9):e1000157.

Pfeffer T et al. (2017). Catecholamines, Not Acetylcholine, Alter Cortical and Perceptual Dynamics in Line with Increased Excitation-Inhibition Ratio. *bioRxiv* 170613.

Polack PO, Friedman J, Golshani P (2013). Cellular Mechanisms of Brain State-Dependent Gain Modulation in Visual Cortex. *Nature Neuroscience* 16(9):1331–1339.

Pouget A, Drugowitsch J, Kepecs A (2016). Confidence and Certainty: Distinct Probabilistic Quantities for Different Goals. *Nature Neuroscience* 19(3):366–374.

Preuschoff K, 't Hart BM, Einhäuser W (2011). Pupil Dilation Signals Surprise: Evidence for Noradrenaline's Role in Decision Making. *Frontiers in Neuroscience* 5:115.

Rabbitt PMA (1968). Repetition Effects and Signal Classification Strategies in Serial Choice-Response Tasks. *Quarterly Journal of Experimental Psychology* 20(3):232–240.

Rahnev D (2017). The Case against Full Probability Distributions in Perceptual Decision Making. *bioRxiv* 108944.

Rahnev D, Denison R (2016). Suboptimality in Perception. *bioRxiv* 060194.

Ratcliff R (1978). A Theory of Memory Retrieval. *Psychological Review* 85(2):59.

Ratcliff R, Childers R (2015). Individual Differences and Fitting Methods for the Two-Choice Diffusion Model of Decision Making. *Decision* 2(4):237–279.

Ratcliff R, McKoon G (2008). The Diffusion Decision Model: Theory and Data for Two-Choice Decision Tasks. *Neural Computation* 20(4):873–922.

Ratcliff R, Tuerlinckx F (2002). Estimating Parameters of the Diffusion Model: Approaches to Dealing with Contaminant Reaction Times and Parameter Variability. *Psychonomic Bulletin & Review* 9(3):438–481.

Read JCA (2015). The Place of Human Psychophysics in Modern Neuroscience. *Neuroscience* 296:116–129.

Reimer J et al. (2014). Pupil Fluctuations Track Fast Switching of Cortical States during Quiet Wakefulness. *Neuron* 84(2):355–362.

Ress D, Backus BT, Heeger DJ (2000). Activity in Primary Visual Cortex Predicts Performance in a Visual Detection Task. *Nature Neuroscience* 3(9):940–945.

Roelfsema PR, de Lange FP (2016). Early Visual Cortex as a Multiscale Cognitive Blackboard. *Annual Review of Vision Science* 2(1):131–151.

Rogers SL et al. (1998). Pharmacokinetic and Pharmacodynamic Profile of Donepezil HCl Following Multiple Oral Doses. *British Journal of Clinical Pharmacology* 46:7.

Roitman JD, Shadlen MN (2002). Response of Neurons in the Lateral Intraparietal Area during a Combined Visual Discrimination Reaction Time Task. *Journal of Neuroscience* 22(21):9475–9489.

Rokem A et al. (2010). Cholinergic Enhancement Increases the Effects of Voluntary Attention but Does Not Affect Involuntary Attention. *Neuropsychopharmacology* 35(13):2538–2544.

Rouder JN, Morey RD, Speckman PL, Province JM (2012). Default Bayes Factors for ANOVA Designs. *Journal of Mathematical Psychology* 56(5):356–374.

Rowan TH (1990). Functional Stability Analysis Of Numerical Algorithms. PhD thesis. Austin: University of Texas.

Sanders JI, Hangya B, Kepecs A (2016). Signatures of a Statistical Computation in the Human Sense of Confidence. *Neuron* 90(3):499–506.

Sara SJ (2009). The Locus Coeruleus and Noradrenergic Modulation of Cognition. *Nature Reviews Neuroscience* 10(3):211–223.

Sauer JM, Ring BJ, Witcher JW (2005). Clinical Pharmacokinetics of Atomoxetine. *Clinical Pharmacokinetics* 44(6):571–590.

Scase MO, Braddick OJ, Raymond JE (1996). What Is Noise for the Motion System? *Vision Research* 36(16):2579–2586.

Schwarz G (1978). Estimating the Dimension of a Model. *The Annals of Statistics* 6(2):461–464.

Shadlen MN, Britten KH, Newsome WT, Movshon JA (1996). A Computational Analysis of the Relationship

between Neuronal and Behavioral Responses to Visual Motion. *Journal of Neuroscience* 16(4):1486–1510.

Shadlen M, Kiani R (2013). Decision Making as a Window on Cognition. *Neuron* 80(3):791–806.

Shadlen M, Shohamy D (2016). Decision Making and Sequential Sampling from Memory. *Neuron* 90(5):927–939.

Shaw AD et al. (2017). Neurophysiologically-Informed Markers of Individual Variability and Pharmacological Manipulation of Human Cortical Gamma. *NeuroImage* 161:19–31.

Siegel M, Buschman TJ, Miller EK (2015). Cortical Information Flow during Flexible Sensorimotor Decisions. *Science* 348(6241):1352–1355.

Siegel M, Engel AK, Donner TH (2011). Cortical Network Dynamics of Perceptual Decision-Making in the Human Brain. *Frontiers in Human Neuroscience* 5.

Siegel M et al. (2008). Neuronal Synchronization along the Dorsal Visual Pathway Reflects the Focus of Spatial Attention. *Neuron* 60(4):709–719.

Siegel M et al. (2006). High-Frequency Activity in Human Visual Cortex Is Modulated by Visual Motion Strength. *Cerebral Cortex* 17(3):732–741.

Spiegelhalter DJ, Best NG, Carlin BP, Van Der Linde A (2002). Bayesian Measures of Model Complexity and Fit. *Journal of the Royal Statistical Society: Series B (Statistical Methodology)* 64(4):583–639.

Spielberg JM et al. (2011). Approach and Avoidance Profiles Distinguish Dimensions of Anxiety and Depression. *Cognitive Therapy and Research* 35(4):359–371.

St. John-Saaltink E, Kok P, Lau HC, de Lange FP (2016). Serial Dependence in Perceptual Decisions Is Reflected in Activity Patterns in Primary Visual Cortex. *Journal of Neuroscience* 36(23):6186–6192.

Stanislaw H, Todorov N (1999). Calculation of Signal Detection Theory Measures. *Behavior Research Methods, Instruments, & Computers* 31(1):137–149.

Steiger JH (1980). Tests for Comparing Elements of a Correlation Matrix. *Psychological Bulletin* 87(2):245.

Steriade M (2000). Corticothalamic Resonance, States of Vigilance and Mentation. *Neuroscience* 101(2):243–276.

Stocker A, Simoncelli EP (2008). A Bayesian Model of Conditioned Perception. *Advances in Neural Information Processing Systems* 20:1409–1416.

Stolk A, Todorovic A, Schoffelen JM, Oostenveld R (2013). Online and Offline Tools for Head Movement Compensation in MEG. *NeuroImage* 68:39–48.

Sugrue LP, Corrado GS, Newsome WT (2004). Matching Behavior and the Representation of Value in the Parietal Cortex. *Science* 304(5678):1782–1787.

Summerfield C, de Lange FP (2014). Expectation in Perceptual Decision Making: Neural and Computational Mechanisms. *Nature Reviews Neuroscience* 15(11):745–756.

Summerfield C, Tsetsos K (2012). Building Bridges between Perceptual and Economic Decision-Making: Neural and Computational Mechanisms. *Frontiers in Neuroscience* 6.

Sutton RS, Barto AG (1998). *Reinforcement Learning: An Introduction*. Cambridge, Massachsetts: A Bradford Book.

Teichert T, Yu D, Ferrera VP (2014). Performance Monitoring in Monkey Frontal Eye Field. *Journal of Neuroscience* 34(5):1657–1671.

Tervo DGR et al. (2014). Behavioral Variability through Stochastic Choice and Its Gating by Anterior Cingulate Cortex. *Cell* 159(1):21–32.

Thaler L, Schütz A, Goodale M, Gegenfurtner K (2013). What Is the Best Fixation Target? The Effect of Target Shape on Stability of Fixational Eye Movements. *Vision Research* 76:31–42.

Tsetsos K, Pfeffer T, Jentgens P, Donner TH (2015). Action Planning and the Timescale of Evidence Accumulation. *PLoS ONE* 10(6):e0129473.

Twomey DM, Kelly SP, O'Connell RG (2016). Abstract and Effector-Selective Decision Signals Exhibit Qualitatively Distinct Dynamics before Delayed Perceptual Reports. *Journal of Neuroscience* 36(28):7346–7352.

Twomey DM, Murphy PR, Kelly SP, O'Connell RG (2015). The Classic P300 Encodes a Build-to-Threshold Decision Variable. *European Journal of Neuroscience* 42(1):1636–1643.

Urai AE, Braun A, Donner TH (2017). Pupil-Linked Arousal Is Driven by Decision Uncertainty and Alters Serial Choice Bias. *Nature Communications* 8:14637.

Urai AE, Murphy PR (2016). Commentary: Sensory Integration Dynamics in a Hierarchical Network Explains Choice Probabilities in Cortical Area MT. *Frontiers in Systems Neuroscience* 10(37).

Urai AE, Pfeffer T (2014). An Action-Independent Signature of Perceptual Choice in the Human Brain. *Journal of Neuroscience* 34(15):5081–5082.

van Bergen RS (2017). Sensory Uncertainty and Response Variability in Human Visual Cortex. PhD thesis. Nijmegen: Radboud University.

van Ravenzwaaij D, Mulder MJ, Tuerlinckx F, Wagenmakers EJ (2012). Do the Dynamics of Prior Information Depend on Task Context? An Analysis of Optimal Performance and an Empirical Test. *Frontiers in Psychology* 3:132.

Van Veen B, van Drongelen W, Yuchtman M, Suzuki A (1997). Localization of Brain Electrical Activity via Linearly Constrained Minimum Variance Spatial Filtering. *IEEE Transactions on Biomedical Engineering* 44(9):867–880.

Varazzani C, San-Galli A, Gilardeau S, Bouret S (2015). Noradrenaline and Dopamine Neurons in the Reward/Effort Trade-off: A Direct Electrophysiological Comparison in Behaving Monkeys. *Journal of Neuroscience* 35(20):7866–7877.

Vinck M, Batista-Brito R, Knoblich U, Cardin J (2015). Arousal and Locomotion Make Distinct Contributions to Cortical Activity Patterns and Visual Encoding. *Neuron* 86(3):740–754.

Wald A (1947). *Sequential Analysis*. Courier Corporation.

Wallis WA (1980). The Statistical Research Group, 1942–1945. *Journal of the American Statistical Association* 75(370):320–330.

Wandell BA, Dumoulin SO, Brewer AA (2007). Visual Field Maps in Human Cortex. *Neuron* 56(2):366–383.

Wang L, Mruczek RE, Arcaro MJ, Kastner S (2015). Probabilistic Maps of Visual Topography in Human Cortex. *Cerebral Cortex* 25(10):3911–3931.

Wang XJ (2002). Probabilistic Decision Making by Slow Reverberation in Cortical Circuits. *Neuron* 36(5):955–968.

Wang XJ (2008). Decision Making in Recurrent Neuronal Circuits. *Neuron* 60(2):215–234.

Warren CM, Nieuwenhuis S, Donner TH (2015). Perceptual Choice Boosts Network Stability: Effect of Neuromodulation? *Trends in Cognitive Sciences* 19(7):362–364.

Weber EH (1846). Tastsinn Und Gemeingefühl. *Handwörterbuch Der Physiologie*. Leipzig: R. Wagner.

Wei Z, Wang XJ (2015). Confidence Estimation as a Stochastic Process in a Neurodynamical System of Decision Making. *Journal of Neurophysiology* 114(1):99–113.

Wernicke JF et al. (2003). Cardiovascular Effects of Atomoxetine in Children, Adolescents, and Adults. *Drug Safety* 26(10):729–740.

Wessel JR, Danielmeier C, Ullsperger M (2011). Error Awareness Revisited: Accumulation of Multimodal Evidence from Central and Autonomic Nervous Systems. *Journal of Cognitive Neuroscience* 23(10):3021–3036.

Wetzels R, Wagenmakers EJ (2012). A Default Bayesian Hypothesis Test for Correlations and Partial Correlations. *Psychonomic Bulletin & Review* 19(6):1057–1064.

White CN, Poldrack RA (2014). Decomposing Bias in Different Types of Simple Decisions. *Journal of Experimental Psychology: Learning, Memory, and Cognition* 40(2):385–398.

Wichmann FA, Hill NJ (2001a). The Psychometric Function: I. Fitting, Sampling, and Goodness of Fit. *Perception & Psychophysics* 63(8):1293–1313.

Wichmann FA, Hill NJ (2001b). The Psychometric Function: II. Bootstrap-Based Confidence Intervals and Sampling. *Perception & Psychophysics* 63(8):1314–1329.

Wiecki TV, Sofer I, Frank MJ (2013). HDDM: Hierarchical Bayesian Estimation of the Drift-Diffusion Model in Python. *Frontiers in Neuroinformatics* 7.

Wimmer K et al. (2015). Sensory Integration Dynamics in a Hierarchical Network Explains Choice Probabilities in Cortical Area MT. *Nature Communications* 6:6177.

Yeung N, Botvinick MM, Cohen JD (2004). The Neural Basis of Error Detection: Conflict Monitoring and the Error-Related Negativity. *Psychological Review* 111(4):931.

Yu AJ, Cohen JD (2008). Sequential Effects: Superstition or Rational Behavior? *Advances in Neural Information Processing Systems* 21:1873–1880.

Yu AJ, Dayan P (2005). Uncertainty, Neuromodulation, and Attention. *Neuron* 46(4):681–692.

Zhang S, Huang CH, Yu AJ (2014). Sequential Effects: A Bayesian Analysis of Prior Bias on Reaction Time and Behavioral Choice. *Proceedings of the 36th Annual Conference of the Cognitive Science Society*.